Substorms, Dipolarization, and Particle Acceleration: Simulations

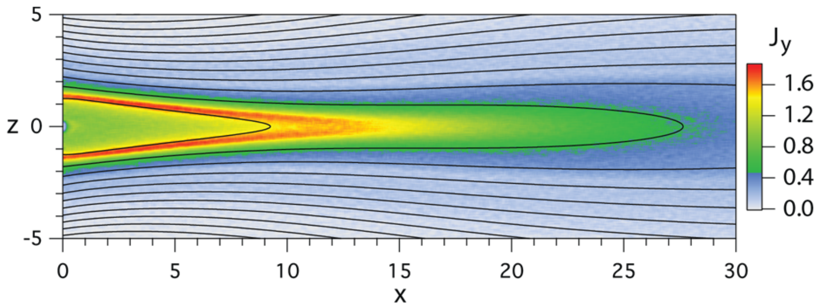

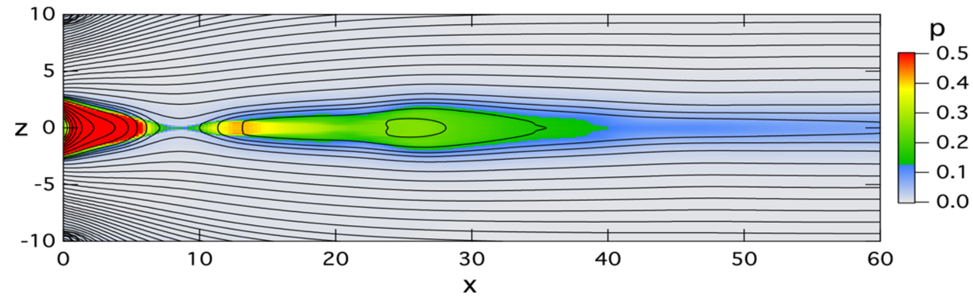

1. Basic plasma physics concepts
2. Substorm phenomenology
3. Thin current sheet formation (Growth phase): MHD, PIC
4. Onset of reconnection in the magnetotail (Onset): PIC
5. Dynamic evolution (Expansion phase): MHD
6. Particle acceleration (Injections): MHD/test particles

Thanks to: Mike Chandler, Bill Daughton, Tom Moore, Michael Hesse, Yi-Hsin Liu, Rumi Nakamura, Antonius Otto, Andrei Runov, Karl Schindler, Xu-Zhi Zhou

1. Basic Charged Particle Motion

Gyration in uniform B field

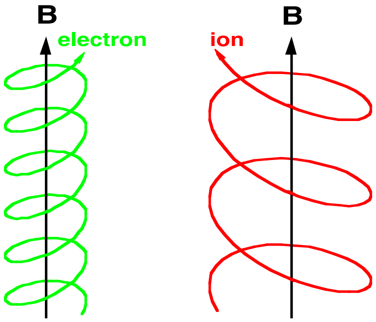

Gyration and drift in uniform E and B fields

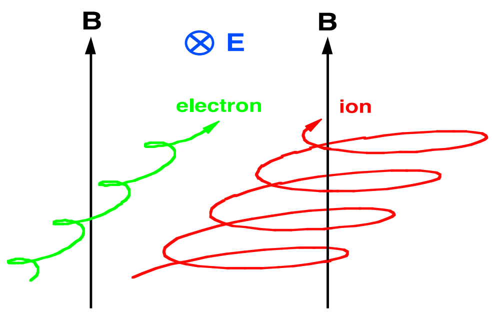

Gyrocenter Drift in Weakly Varying Fields

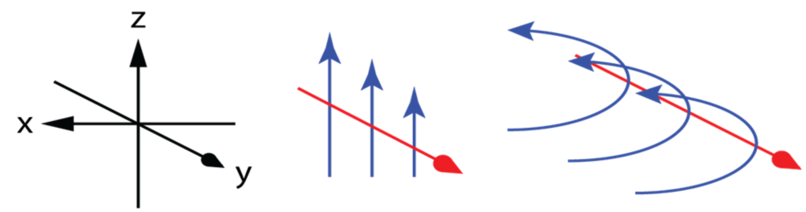

$$\omega_c = \frac{qB}{m}$$ gyrofrequency

$$a_c = \frac{w_\perp}{\omega_c}$$ Larmor radius

$$\mathbf{u}_E = \frac{\mathbf{E}\times\mathbf{B}}{B^2}$$

E × B drift

$$\mathbf{u}_\perp = \frac{\mathbf{E}\times\mathbf{B}}{B^2} + \frac{\mu}{q}\frac{\mathbf{B}\times\nabla B}{B^2} + \frac{mu_\parallel}{q}\frac{\mathbf{B}\times d\mathbf{b}/dt}{B^2}$$

$$\mathbf{b} = \frac{\mathbf{B}}{B} \qquad \mu = \frac{mw_\perp^2}{2B}$$ magnetic moment

"Frozen-in Fields" & Reconnection

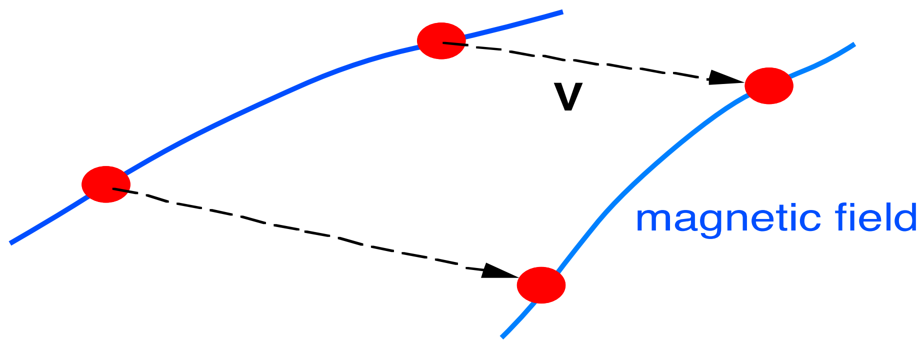

Ideal MHD, $\mathbf{E} + \mathbf{V} \times \mathbf{B} = 0$,

"Frozen-in Fields"

Plasma elements stay connected
No change in Topology
No flow across topological boundary (separatrix)

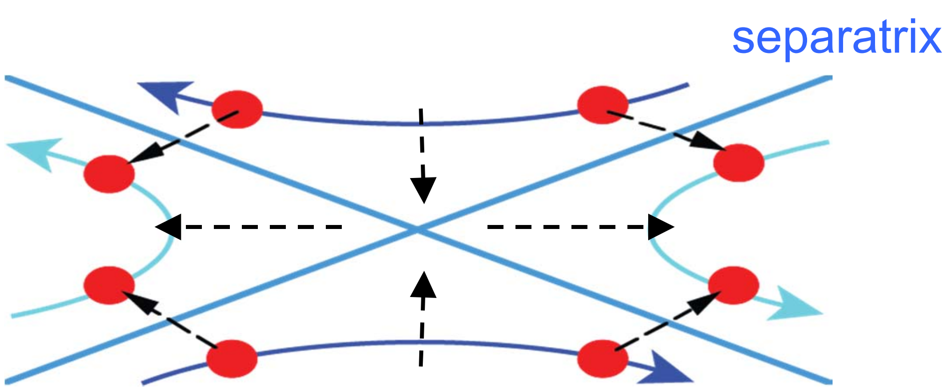

Reconnection

Local violation of ideal MHD
New magnetic connections
Enables change in topology
Enables flow across separatrix
Enables conversion of magnetic to particle energy

Basic Instabilities

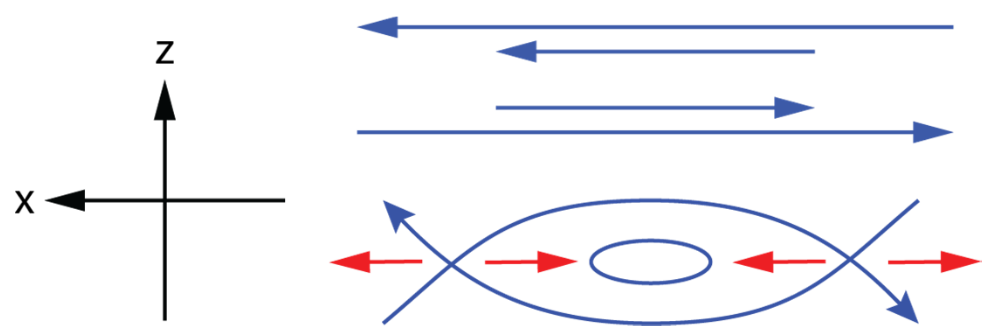

Tearing instability
in thin current sheets,
forming magnetic islands,
initiates reconnection

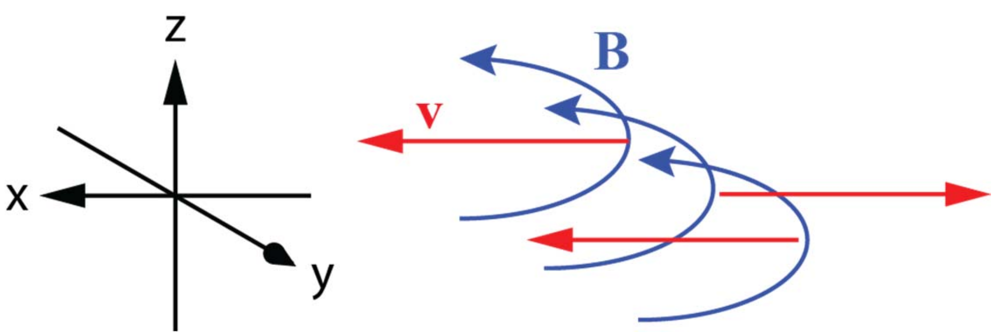

Ballooning/
Interchange mode
driven by grad P
in curved magnetic field

Basic Approaches

Single particle motion

$\mathbf{E}$ & $\mathbf{B}$ given (e.g. by MHD): test particle

$\mathbf{E}$ & $\mathbf{B}$ derived from all particles: e.g., Particle In Cell simulation

$$\frac{dm\mathbf{u}}{dt} = q(\mathbf{E} + \mathbf{u} \times \mathbf{B})$$

Fluid motion (MHD)

$$\partial\rho/\partial t = -\nabla \cdot \rho\mathbf{v}$$

$$\rho\, d\mathbf{v}/dt = -\nabla p + \mathbf{j} \times \mathbf{B}$$

$$\mathbf{E} + \mathbf{v} \times \mathbf{B} = \eta\mathbf{j}$$

$$dp / dt = -\gamma p \nabla \cdot \mathbf{v} + (\gamma - 1)\eta j^2$$

$$\partial\mathbf{B} / \partial t = -\nabla \times \mathbf{E}$$

$$\nabla \times \mathbf{B} = \mu_0 \mathbf{j}$$

2. Magnetosphere and Substorms

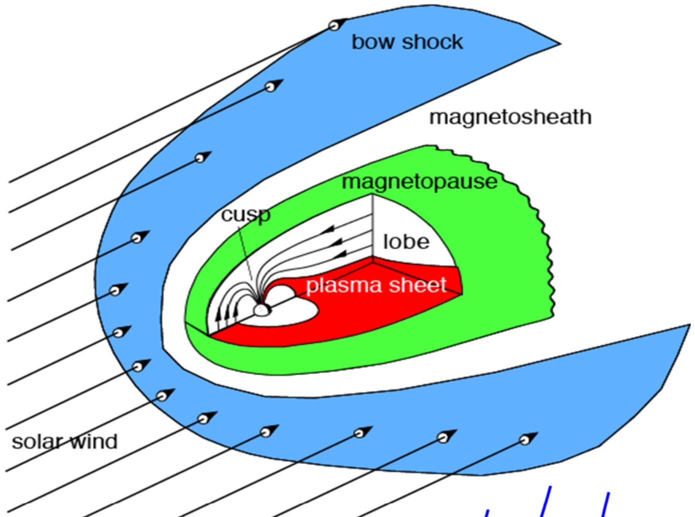

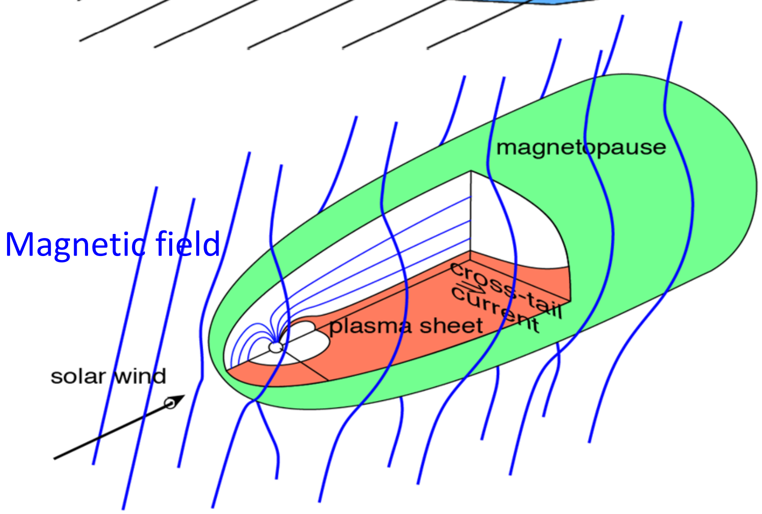

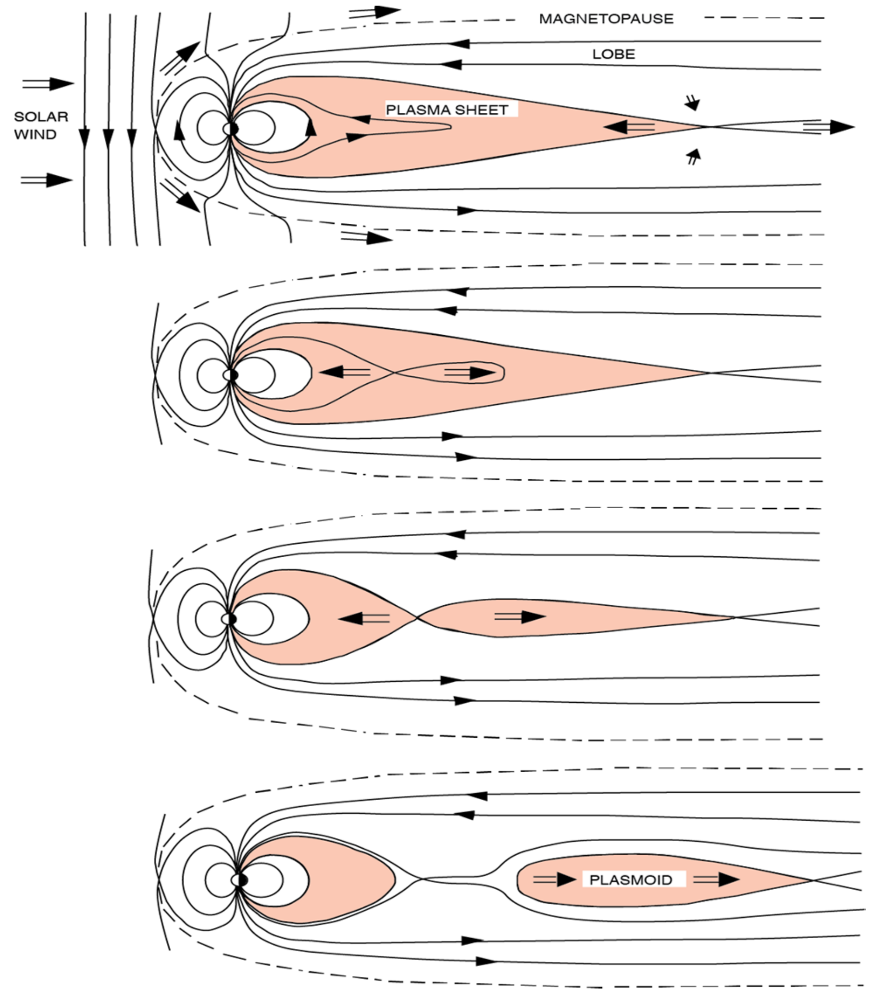

Plasmoid Ejection & Substorm Current Wedge

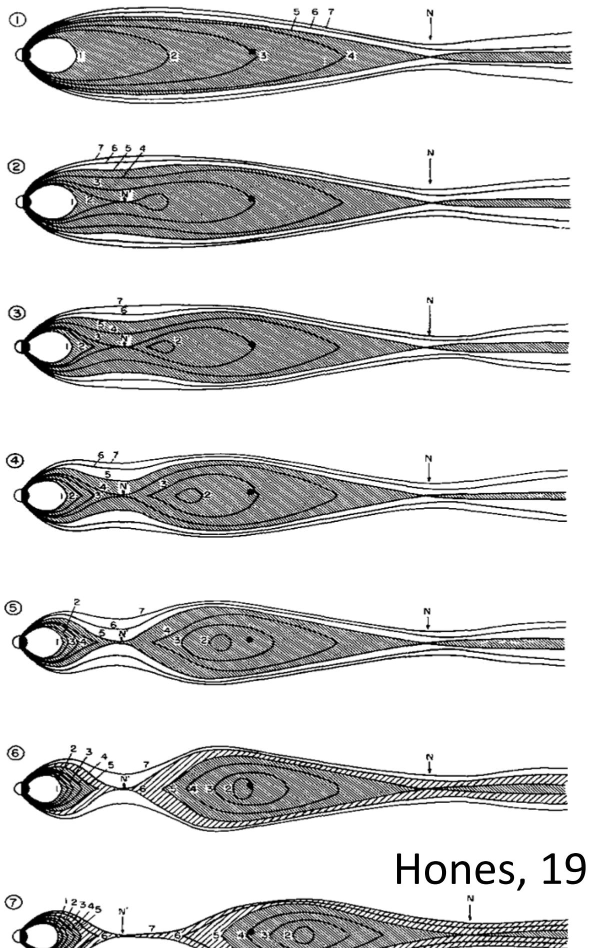

Hones, 1977

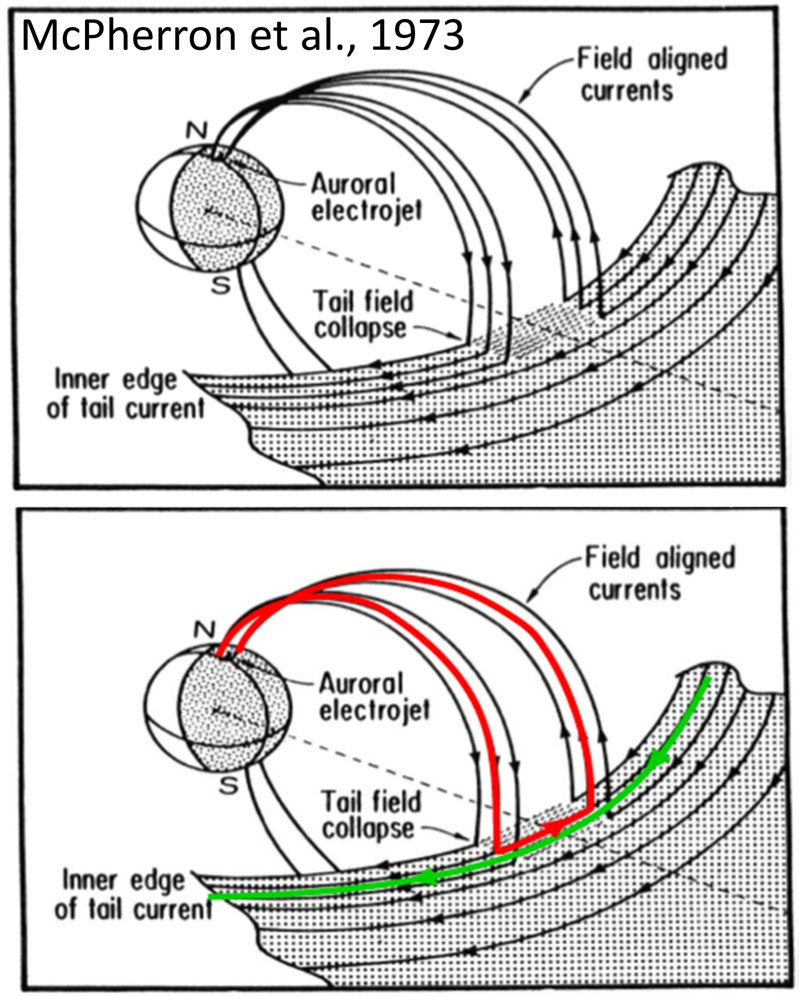

McPherron et al., 1973

3. Growth Phase: Thin Current Sheet Formation

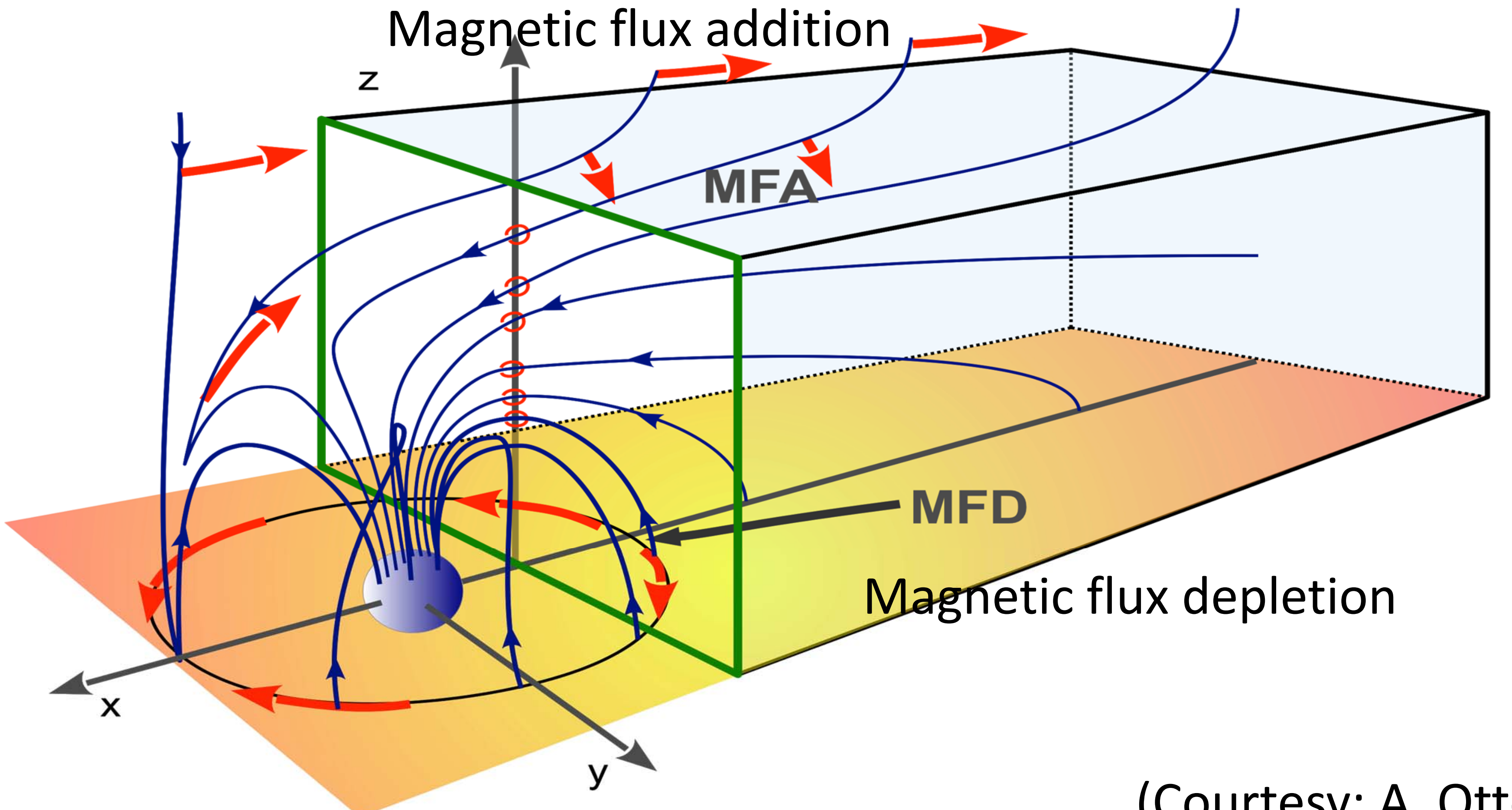

(Courtesy: A. Otto)

4. Onset of Reconnection (PIC Simulations): Slow Deformation of Stable Tail

Initial state, 2D Tail: $L_z = 2\ d_i$, $B_z = 0.05\ B_0$

-> stability to tearing (e.g., Brittnacher et al., 1995; Daughton, 1999)

Monotonic entropy function, $S = P^{1/\gamma}V$

-> stability to ballooning/interchange -> MHD stability (e.g., Schindler, 2007)

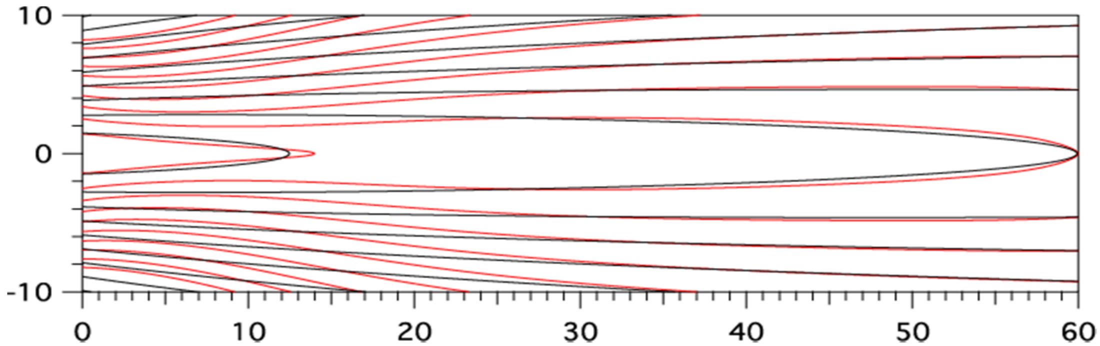

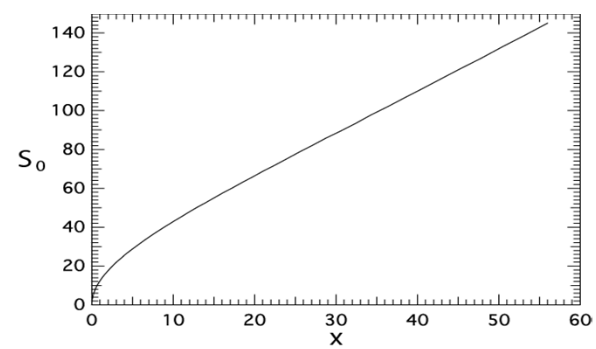

Finite deformation of tail equilibrium by temporally limited external inflow of magnetic flux; vary amplitude a, m_I/m_e up to 1836

Formation of thin embedded current sheet – may or may not lead to onset, loss of equilibrium

(Hesse & Schindler, 2001; Birn & Hesse, 2014; Liu, Birn, Daughton, Hesse, & Schindler, 2014)

PIC Simulations: Deformation of Stable Tail (Liu et al.)

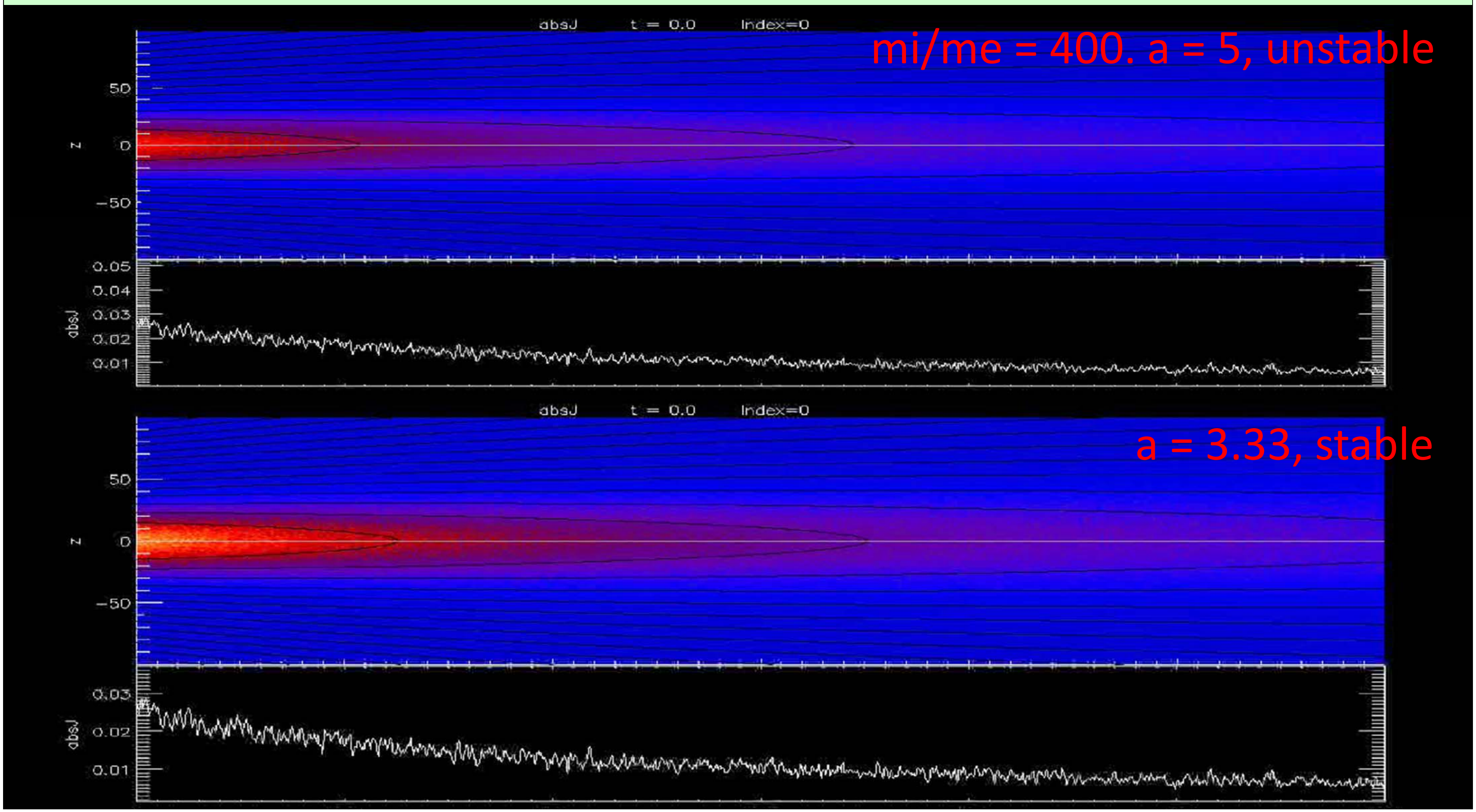

Onset, Evolution Dependence on Mass Ratio

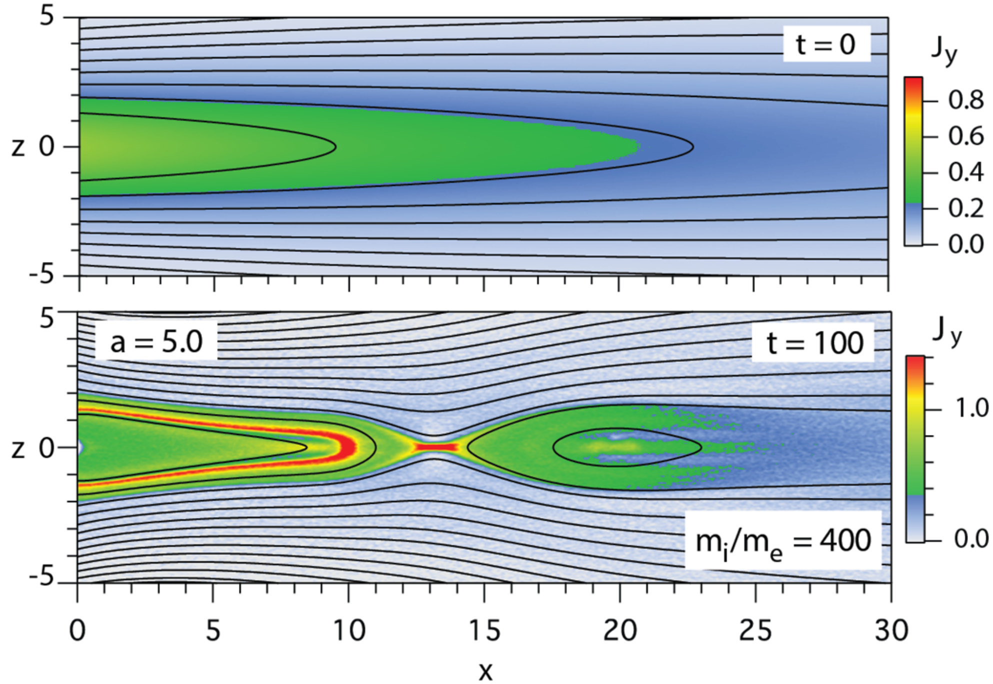

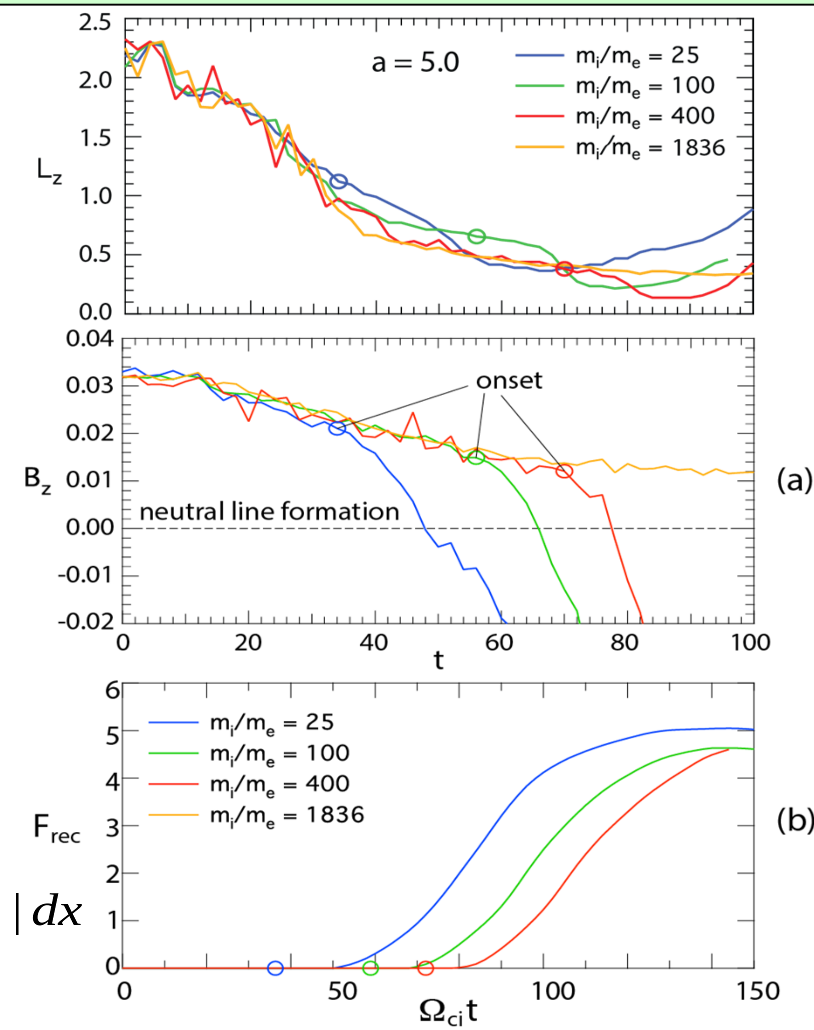

$$F_{rec} = \int_{Bz<0} | B_z | \, dx$$

Entropy $S = \int p^{1/\gamma} ds / B$

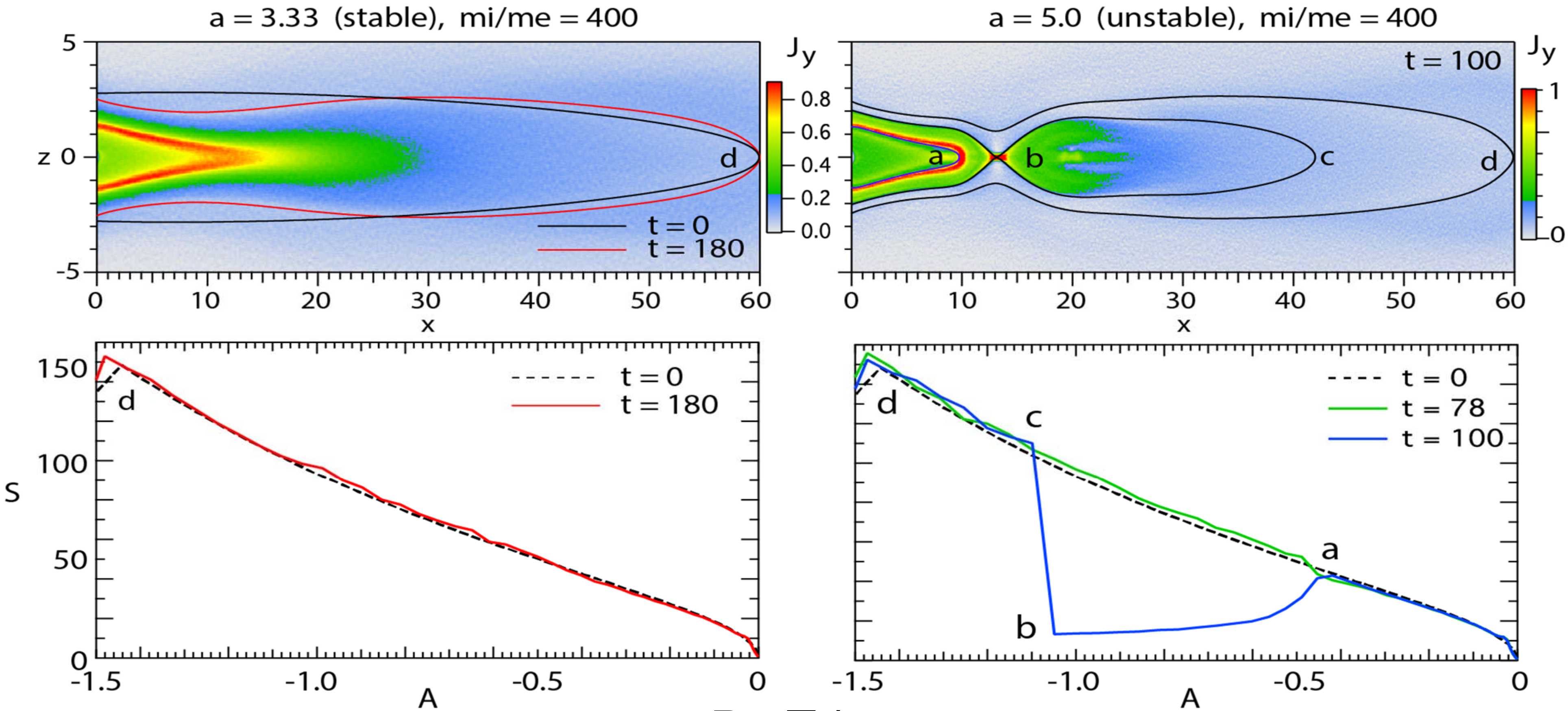

$\mathbf{B} = \nabla A \times \mathbf{e}_y$

Ballooning stable before onset of tearing, unstable after plasmoid loss

Summary: Onset & Early Evolution

- CS thinning, onset of tearing instability depend on the amount of deformation, localization (continuous driving not necessary)
- Onset requires both (**local**) thinning and reduction of Bz
  (go together under external deformation)
- Early, stable evolution independent of mass ratio, consistent with ideal MHD
- Onset of instability depends on mass ratio (electron tearing)
- Unstable modes rise even before Bz changes sign
- Evolution after x-line formation independent of mass ratio
- PIC (2D) evolution conserves entropy integral prior to onset:
  B/I stability before onset of tearing, but plasmoid loss changes entropy integral, may enable B/I instability

5. Dynamic Evolution: 3D MHD Simulation

Initial driving as in PIC, onset of reconnection by imposing resistivity

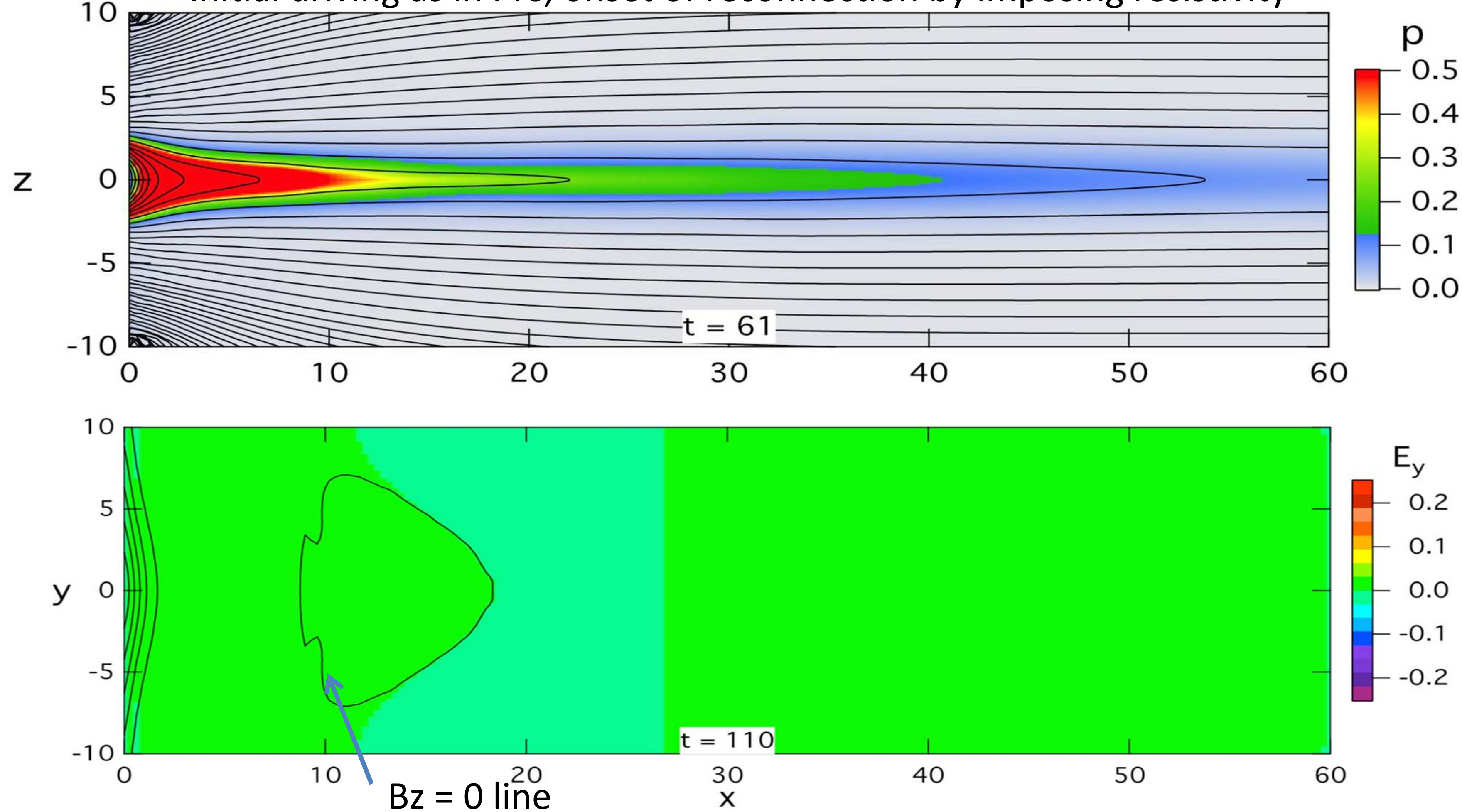

3D MHD Simulation & Observations

THEMIS observations
(Panov et al., 2010)

MHD simulations
(Birn et al., 2011)

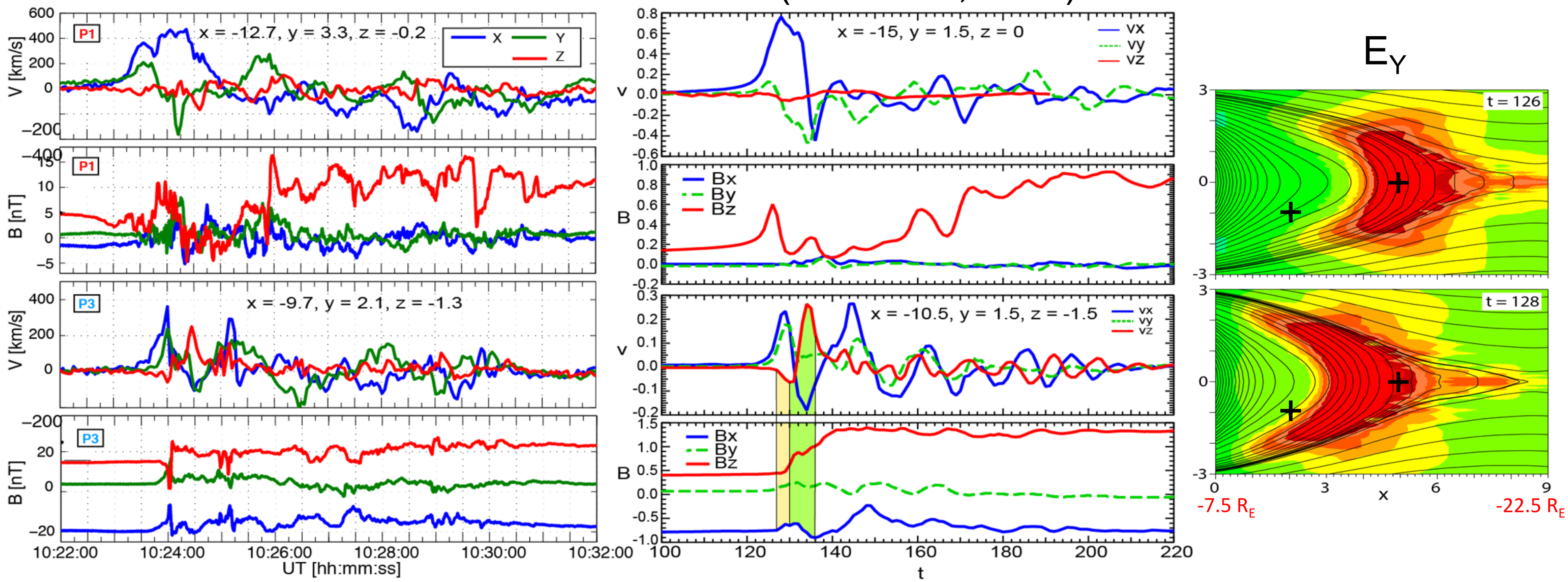

MHD reproduces bouncing, pulsating, dipolarization sequences

Entropy and Flow in 3D MHD Simulation

$$S = \int p^{1/\gamma} ds / B$$

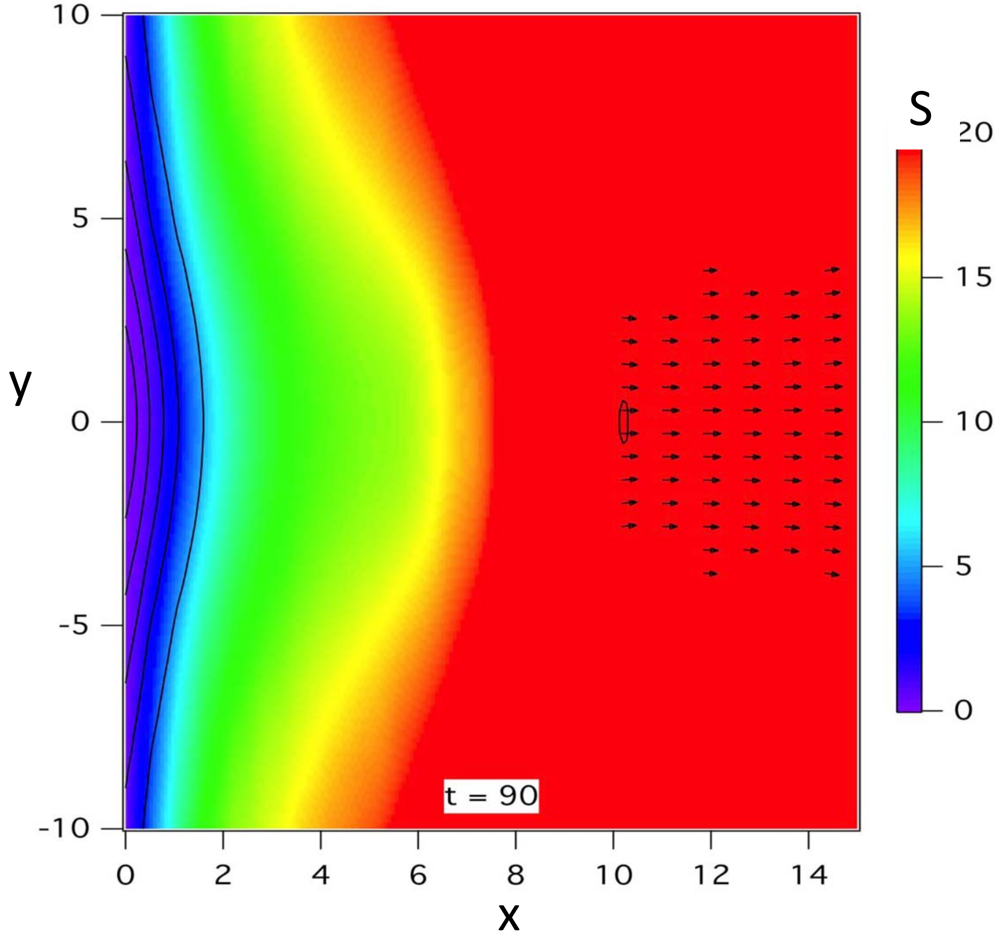

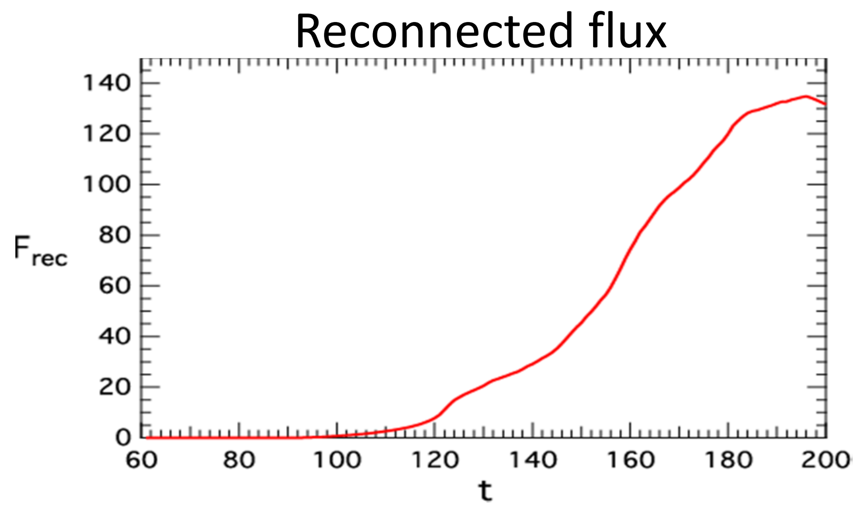

Onset of Fast Reconnection in 3D MHD

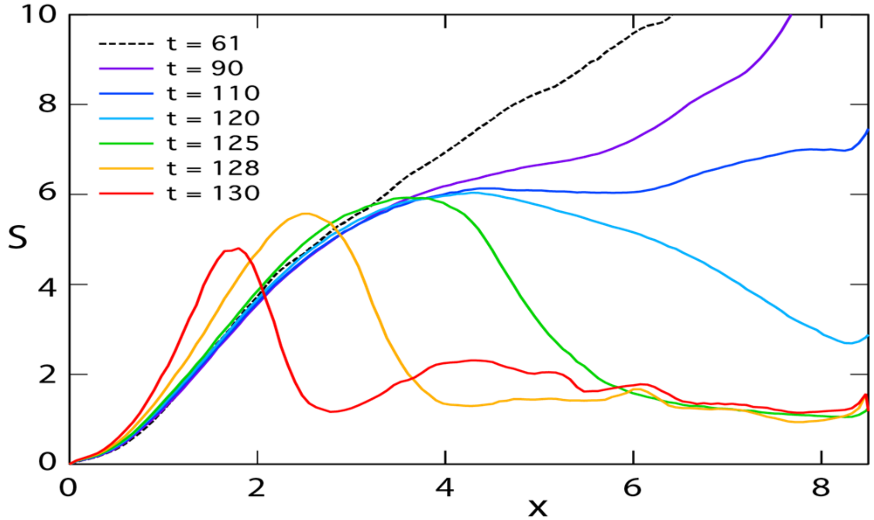

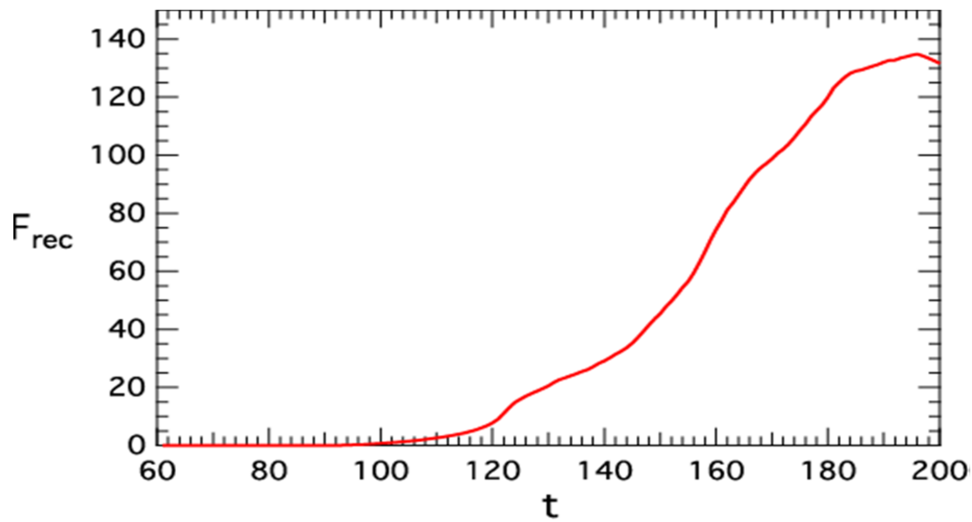

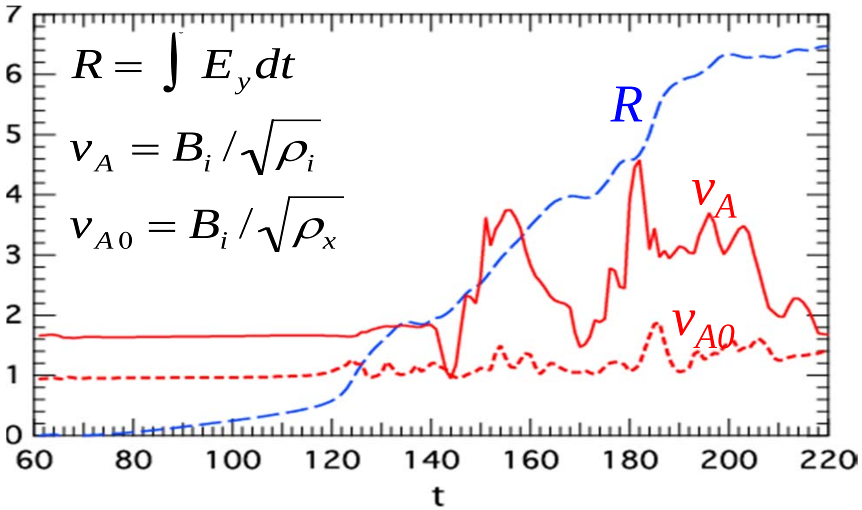

Entropy loss enables Ballooning/interchange instability, faster reconnection

Build-up of Substorm Current Wedge

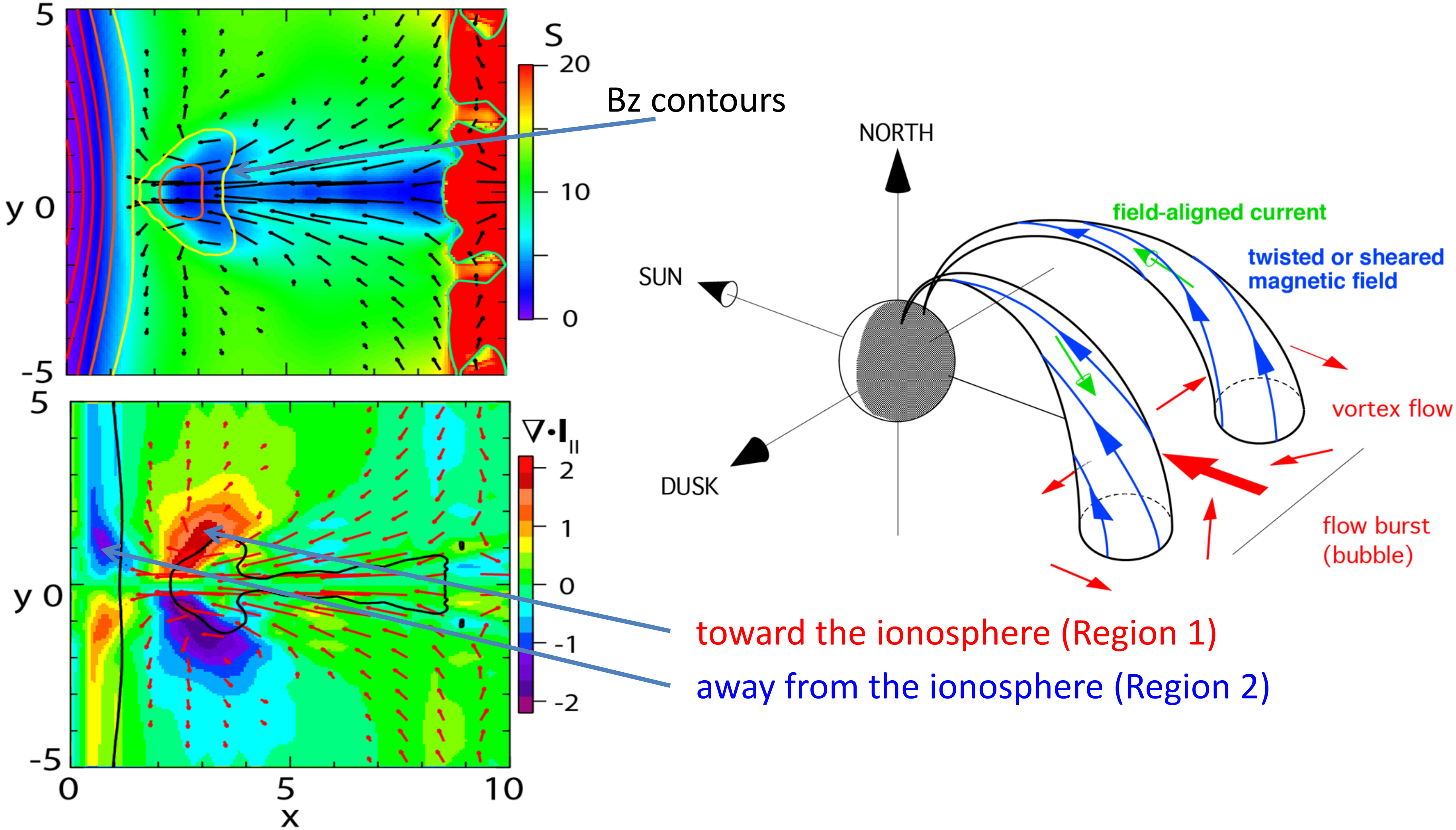

Modifications of Substorm Current Wedge

Loops 4 & 5

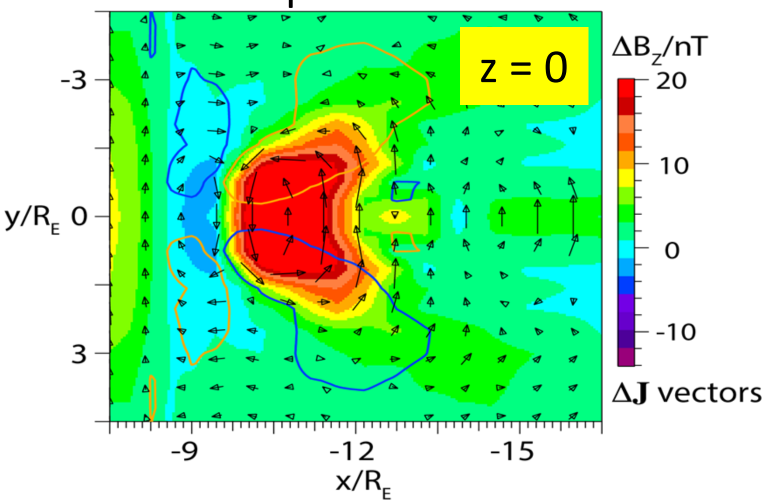

Loop 2

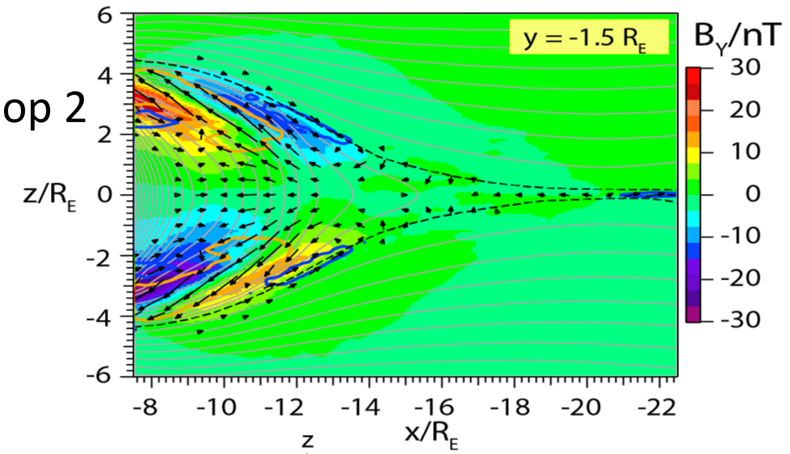

Loops 1 & 3

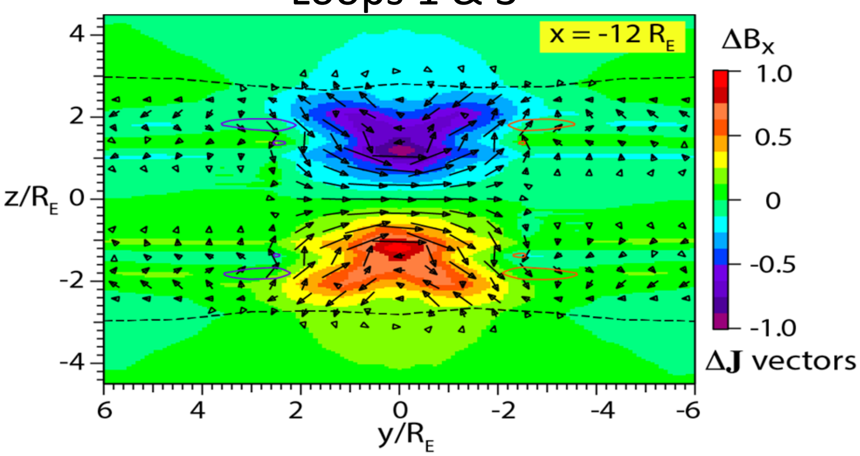

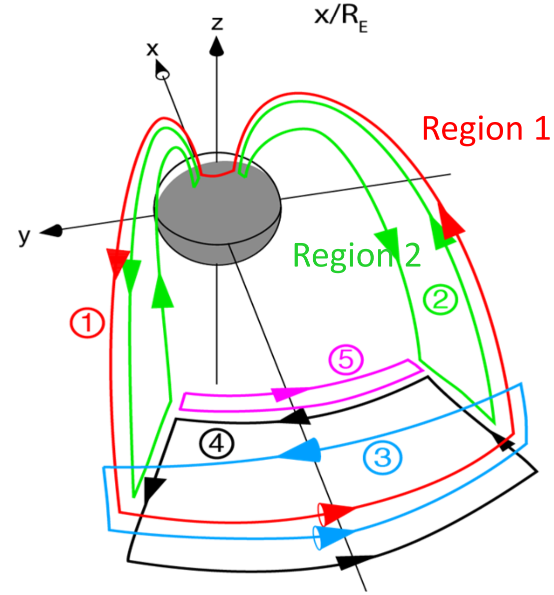

Evolution of SCW : $J_{\|}, I_{\|}$ at x = 0 (-7.5 R_E)

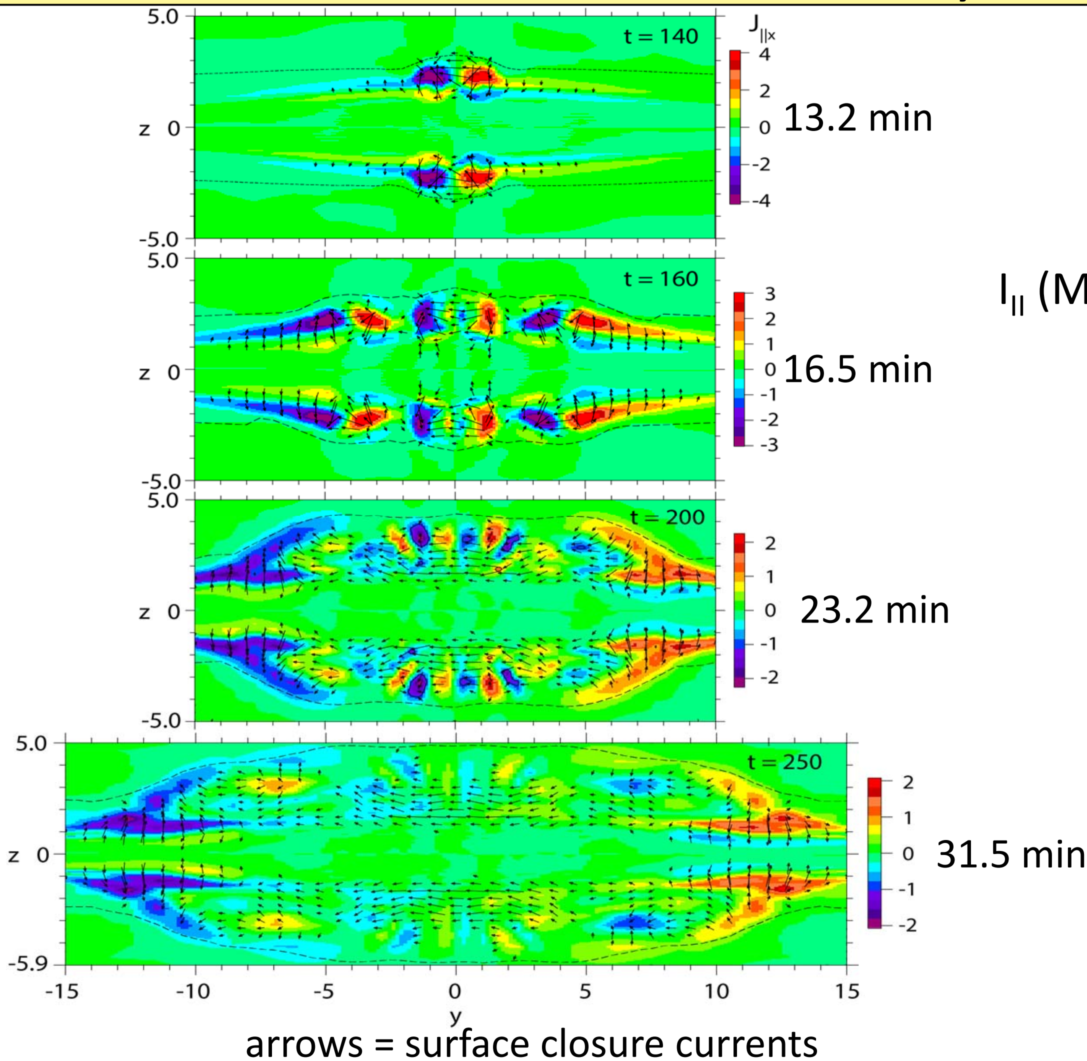

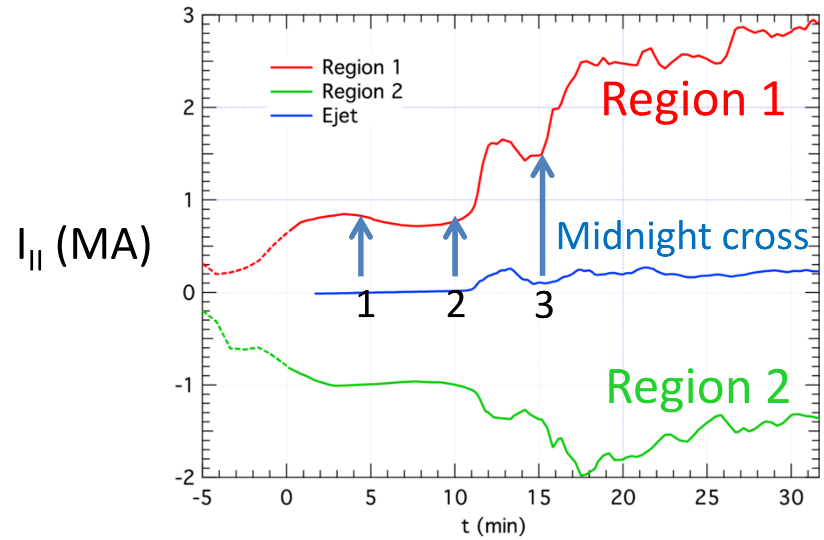

1. Onset of reconnection,
2. Onset of fast reconnection,
3. Additional flow bursts

Summary, MHD Results

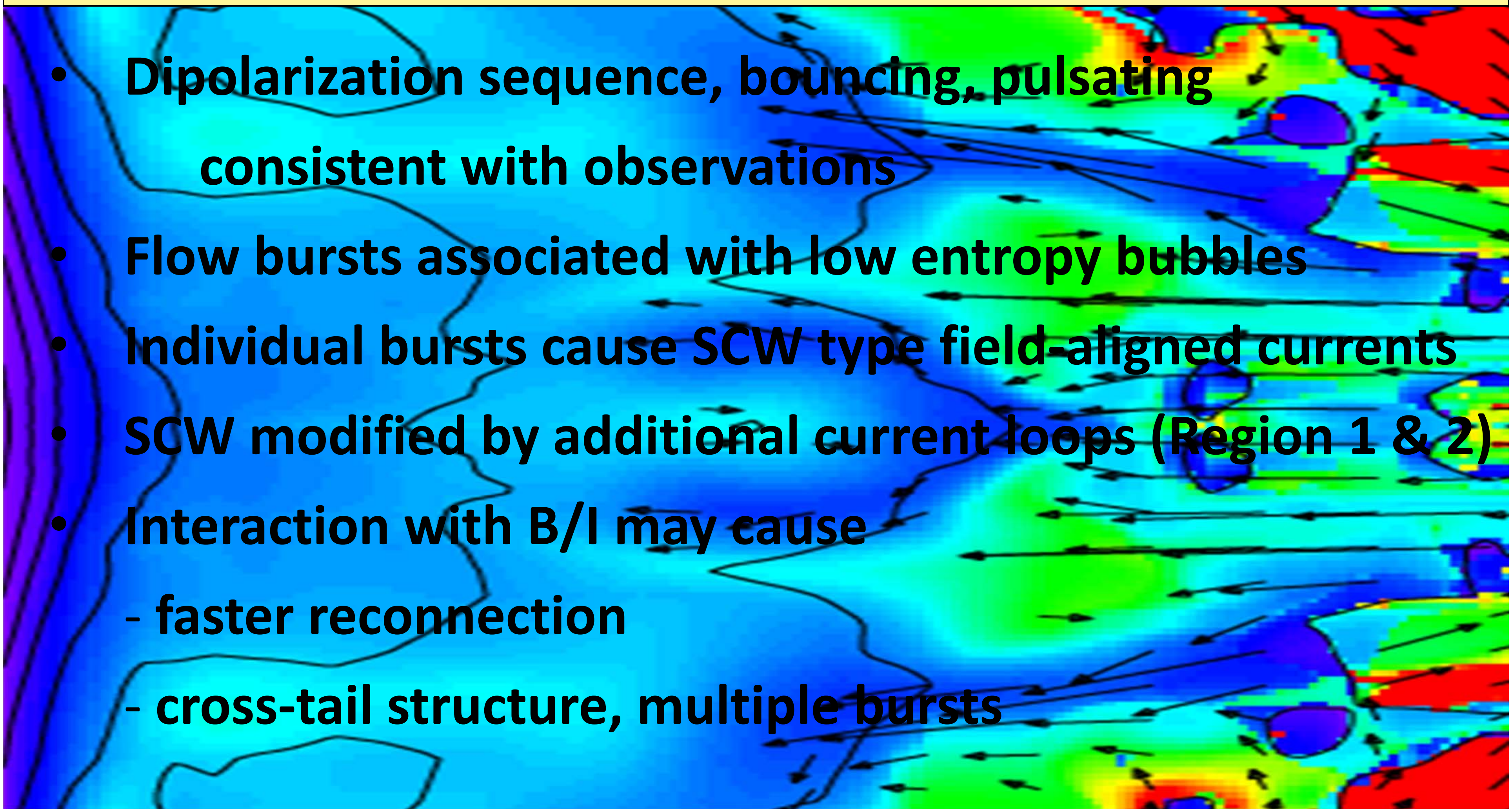

- Dipolarization sequence, bouncing, pulsating
  consistent with observations
- Flow bursts associated with low entropy bubbles
- Individual bursts cause SCW type field-aligned currents
- SCW modified by additional current loops (Region 1 & 2)
- Interaction with B/I may cause
  - faster reconnection
  - cross-tail structure, multiple bursts

6. Particle Acceleration in Dipolarization Events

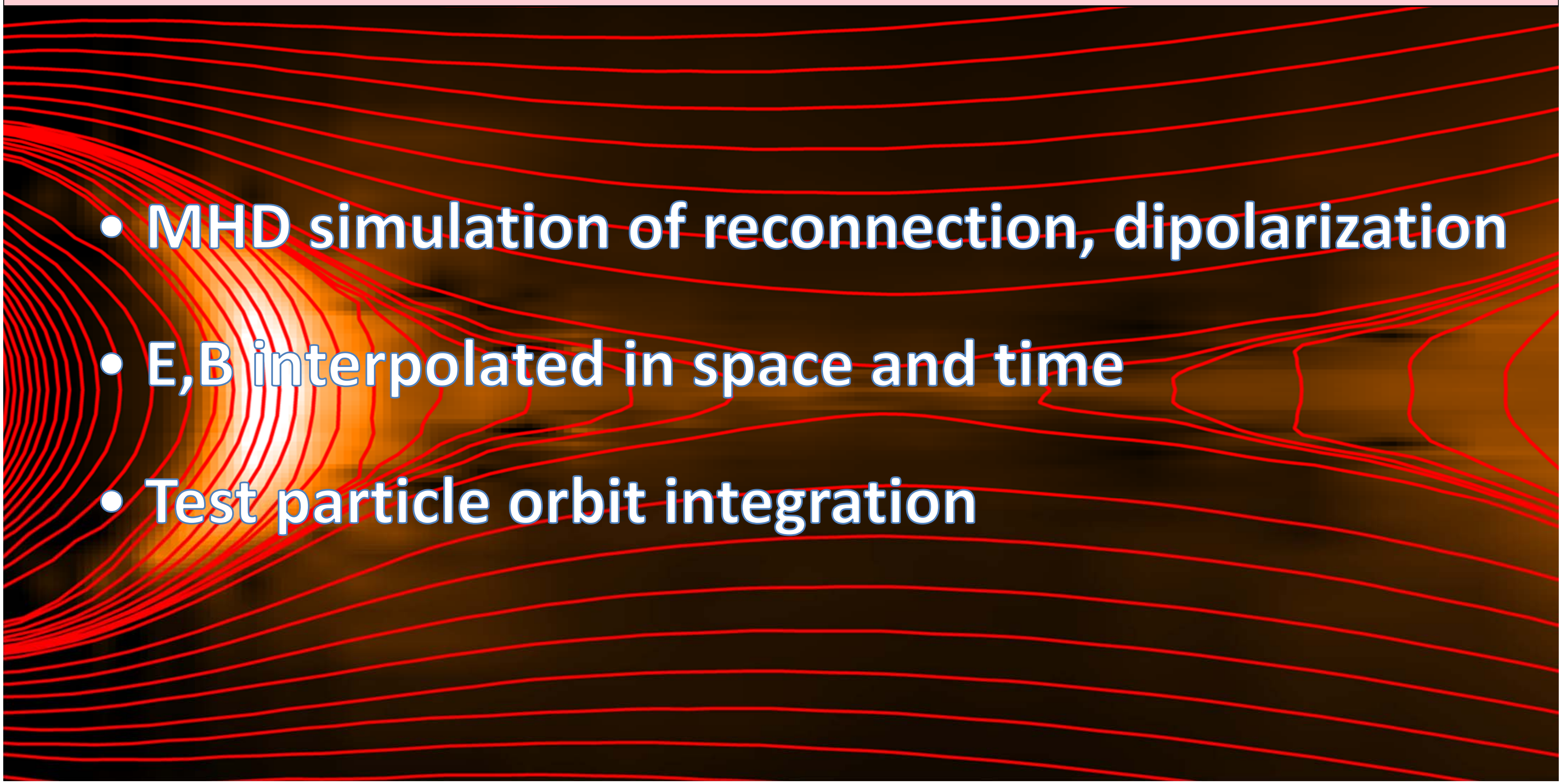

- MHD simulation of reconnection, dipolarization
- E,B interpolated in space and time
- Test particle orbit integration

Test Particle Tracing in MHD Fields

Using time-dependent E & B fields, interpolated in space and time
(cubic spline in space; monotonicity conserving algorithm; avoid fake $E_{||}$)
Backward tracing from final destination to origin at boundary or initial state
Impose f at origin = f at final location (Liouville mapping: Df/Dt = 0)
Reflection at near-Earth boundary accounts for delay from mirroring closer to Earth, based on estimates from orbits in Tsyganenko field model.

Full equation of motion in strongly varying or weak fields (always for ions)

$$\frac{dm\mathbf{u}}{dt} = q(\mathbf{E} + \mathbf{u} \times \mathbf{B})$$

Gyrocenter drift in weakly varying fields (μ_{rel} conserved)

$$\mathbf{v}_\perp = \mathbf{v}_E + \frac{\mu}{q}\frac{\mathbf{B} \times \nabla B}{B^2} + \frac{mv_\parallel^2}{q}\frac{\mathbf{B}}{B^2} \times (\mathbf{b} \bullet \nabla \mathbf{b}) \qquad \mathbf{v}_E = \frac{\mathbf{E} \times \mathbf{B}}{B^2}$$

$$\frac{dmv_\parallel}{dt} = qE_\parallel - \mu \mathbf{b} \bullet \nabla B + mv_\parallel(\mathbf{v}_E + \mathbf{v}_{\nabla B}) \bullet (\mathbf{b} \bullet \nabla \mathbf{b}) \qquad \mathbf{b} = \frac{\mathbf{B}}{B}$$

$$m = \gamma m_0 \qquad \mu = \frac{\mu_{rel}}{\gamma} \qquad \mu_{rel} = \frac{p_\perp^2}{2m_0 B} \qquad \gamma = \frac{1}{\sqrt{1-(v/c)^2}}$$

Transition based on adiabaticity parameter ($\kappa^2 = r_{curv}/a_{gyr}$)

Basic Acceleration Mechanisms

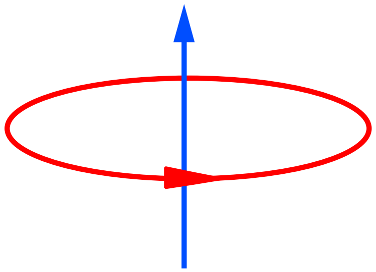

Betatron acceleration $\mu = \frac{m v_\perp^2}{2\,B}$

increasing B -> increasing $v_\perp$
ExB drift in direction of grad B
grad B drift in direction of **E**

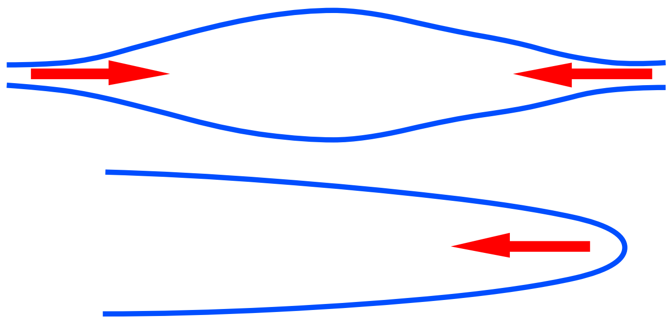

Fermi acceleration
mirroring (type A)
slingshot (type B):
ExB drift in direction of curvature vector
curvature drift in direction of **E**

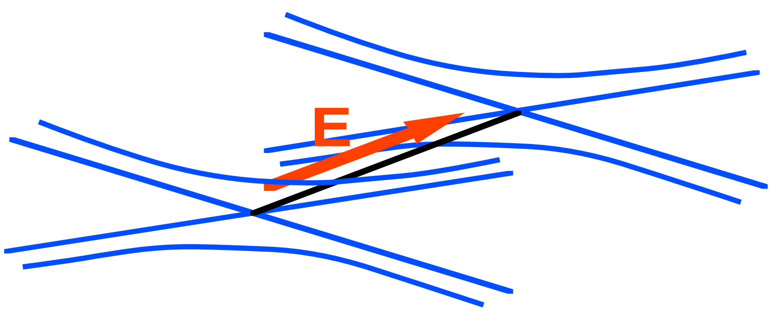

Neutral line acceleration
Direct acceleration

unmagnetized particles

Ion Acceleration, Sample

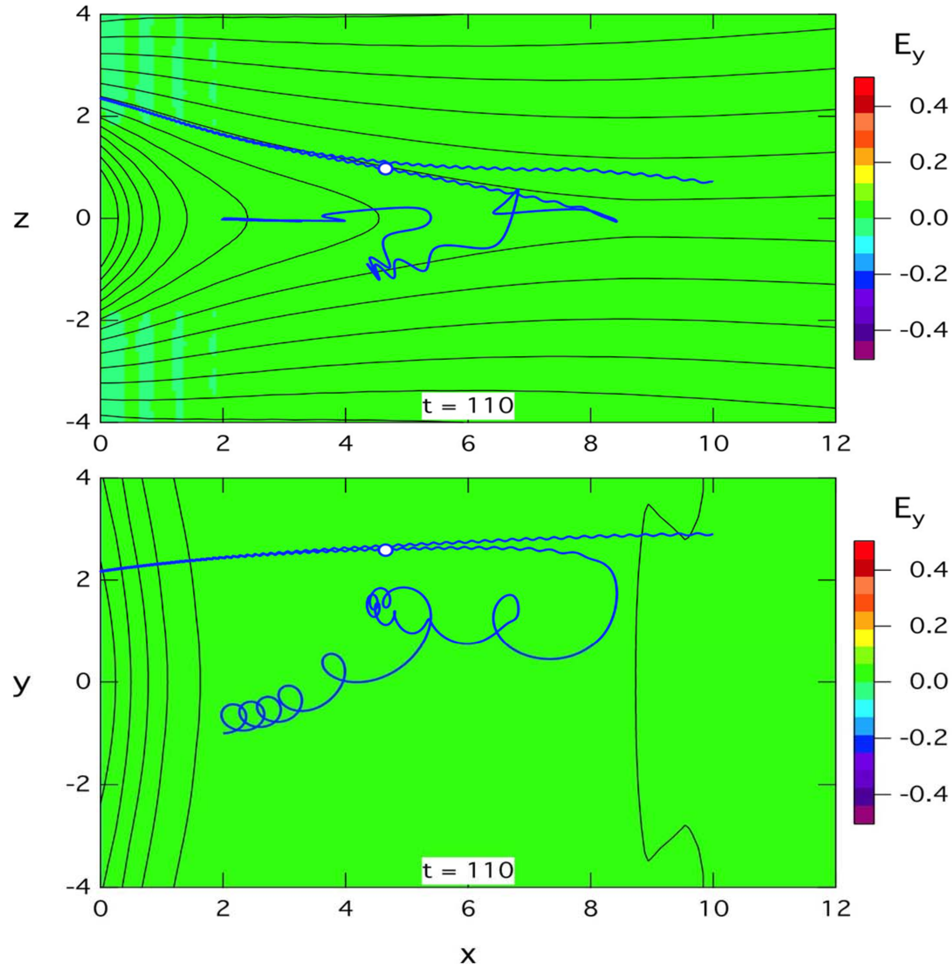

Proton, final energy ≈ 86 keV

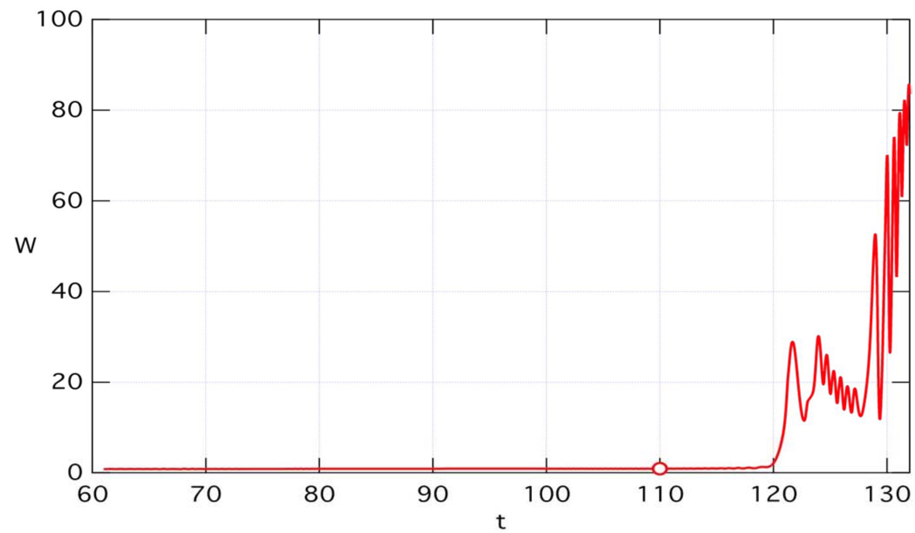

Entry via reconnection

Sample Electron Acceleration, Drift Path

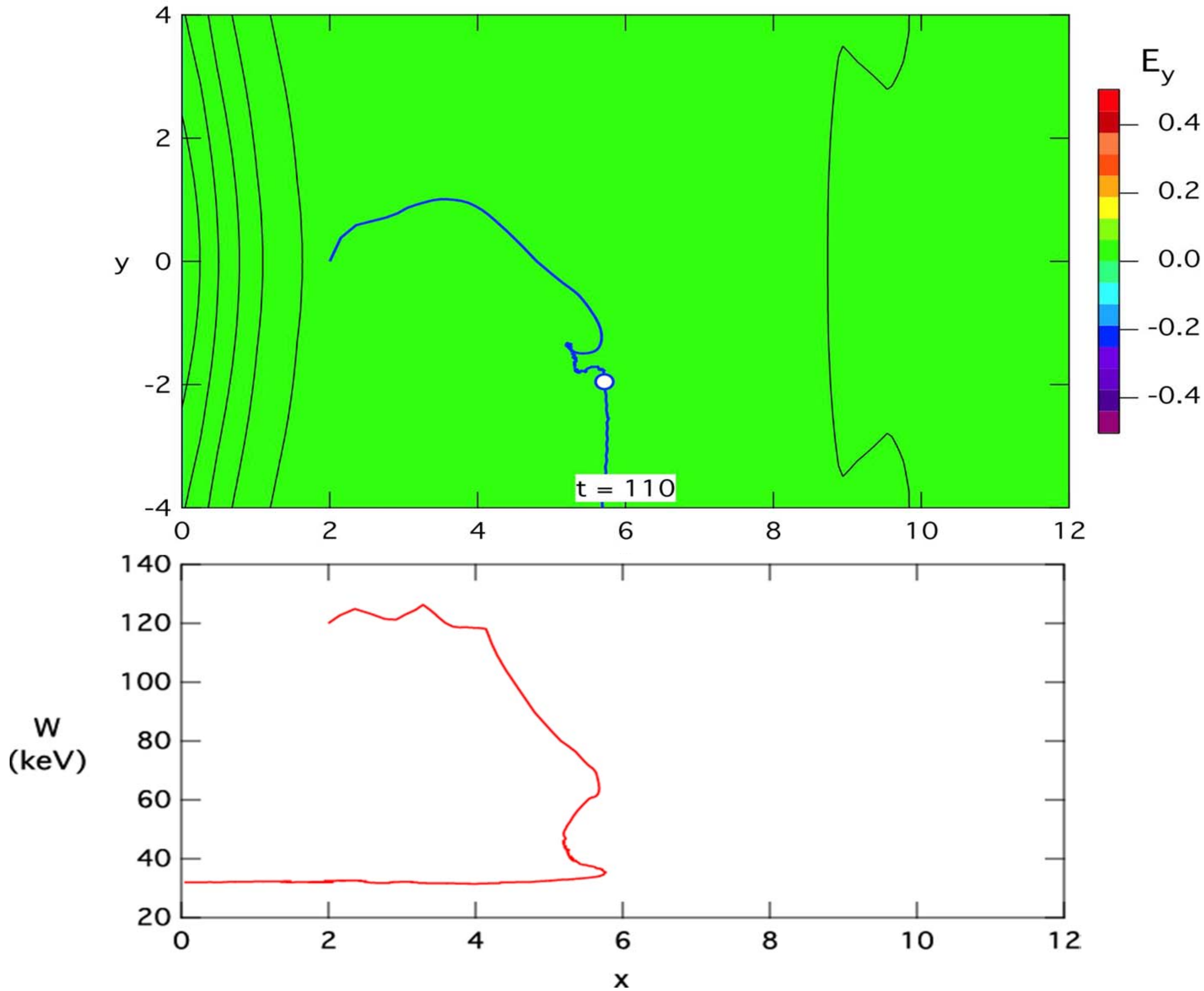

Electron,
final energy ≈ 120 keV

Entry via cross-tail drift,
Betatron acceleration

Electron Fermi Acceleration (small pitch angle)

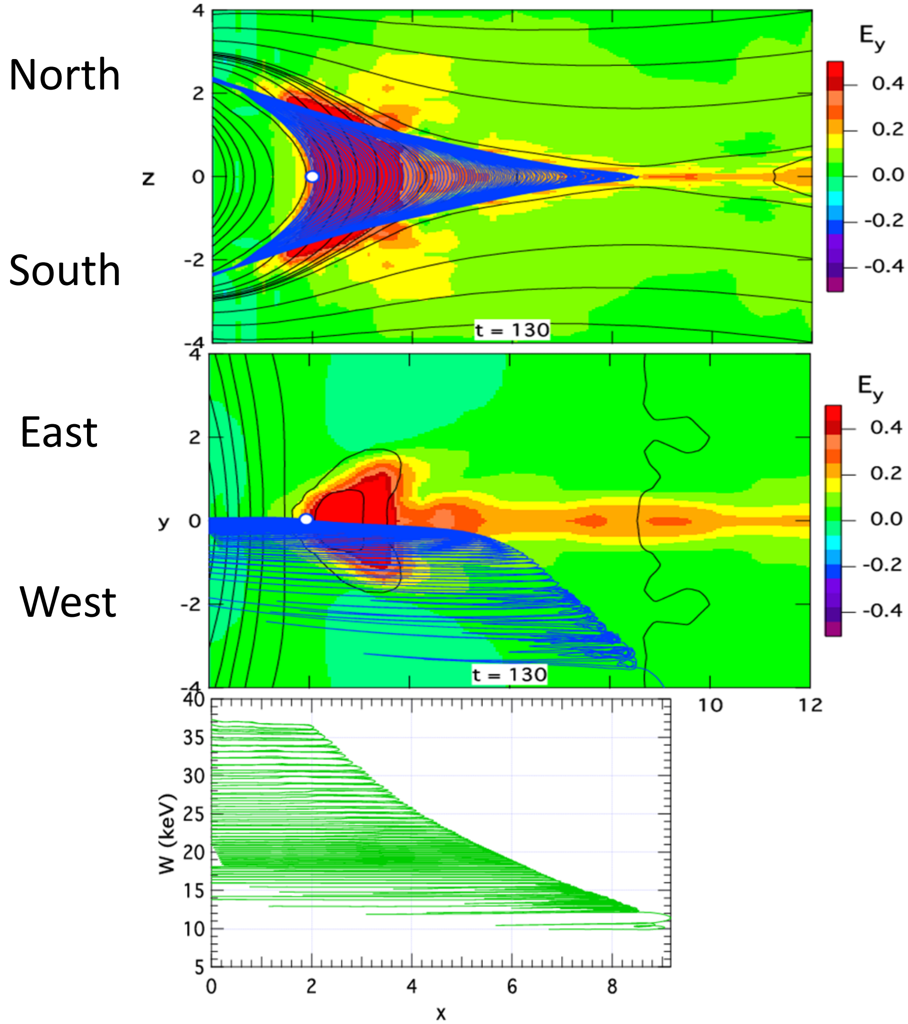

Entry by reconnection or cross-tail drift, earthward E×B drift + cross-tail curvature drift

Repeated energy gain at equatorial crossings between mirroring (current sheet acceleration - 1st order Fermi, type B)

Overview: 47 keV Upward Proton Fluxes

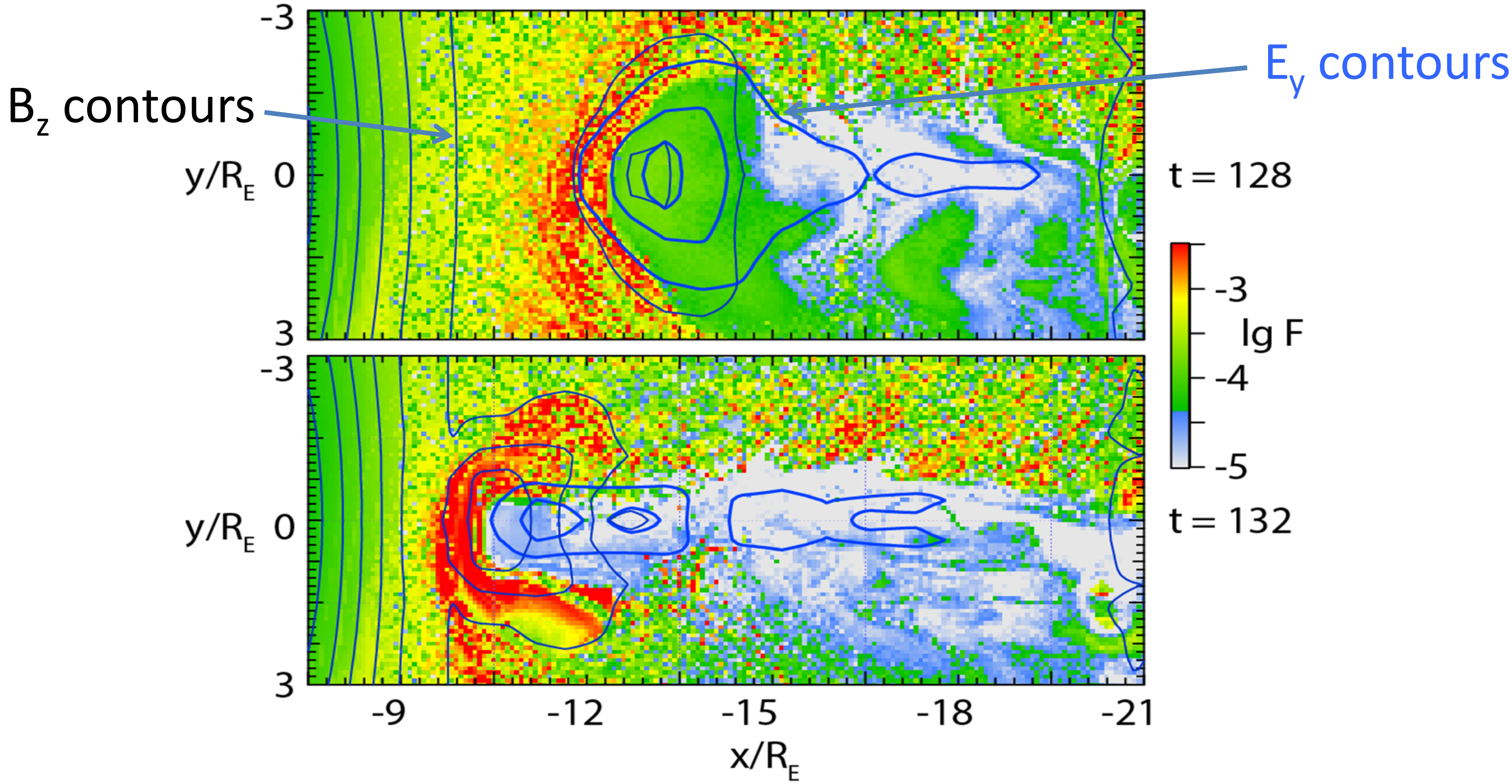

Overview: 47 keV Earthward Proton Fluxes

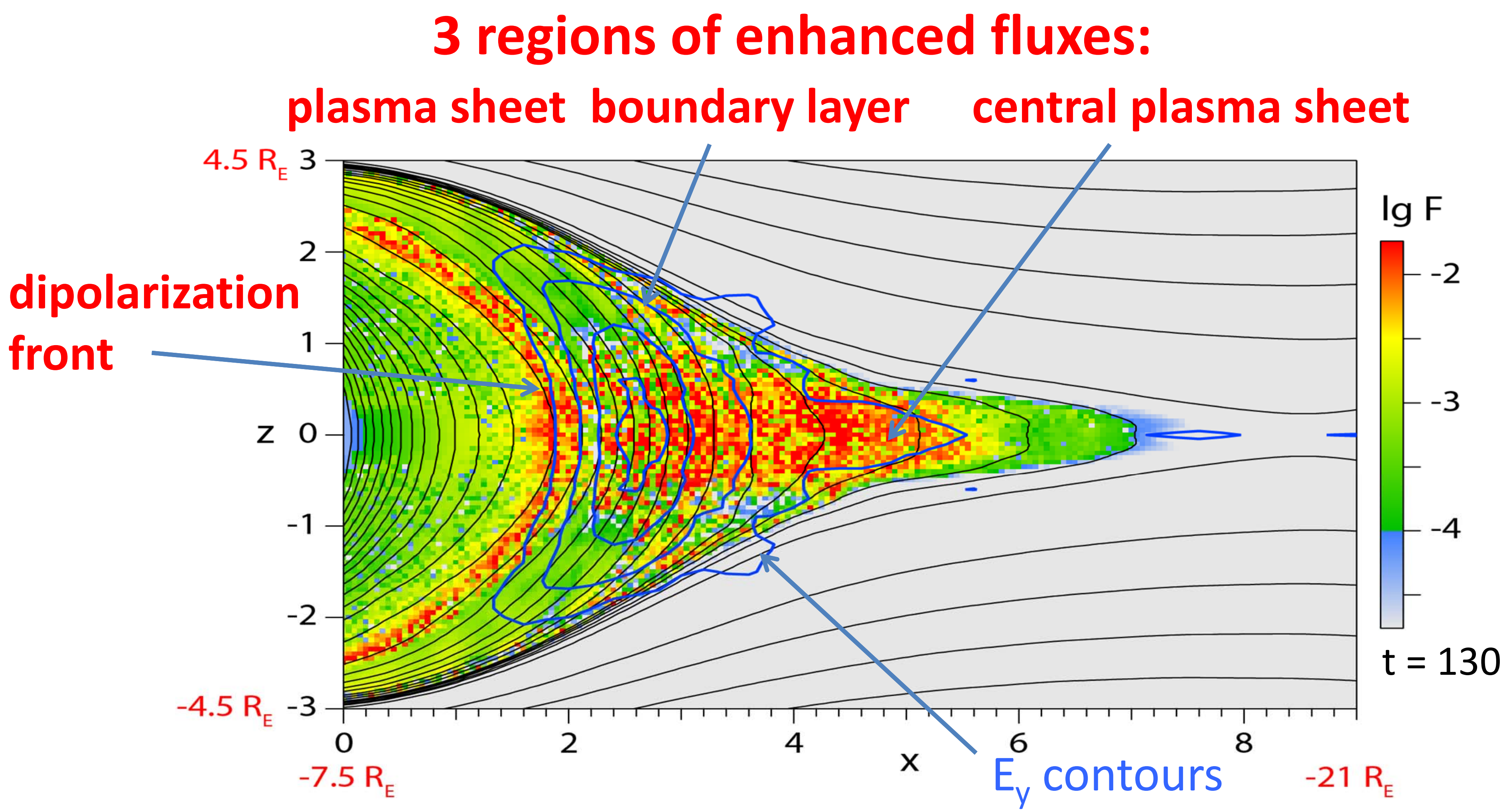

Simulated Event Overview, Near Tail Reconnection

Ey-field, MHD

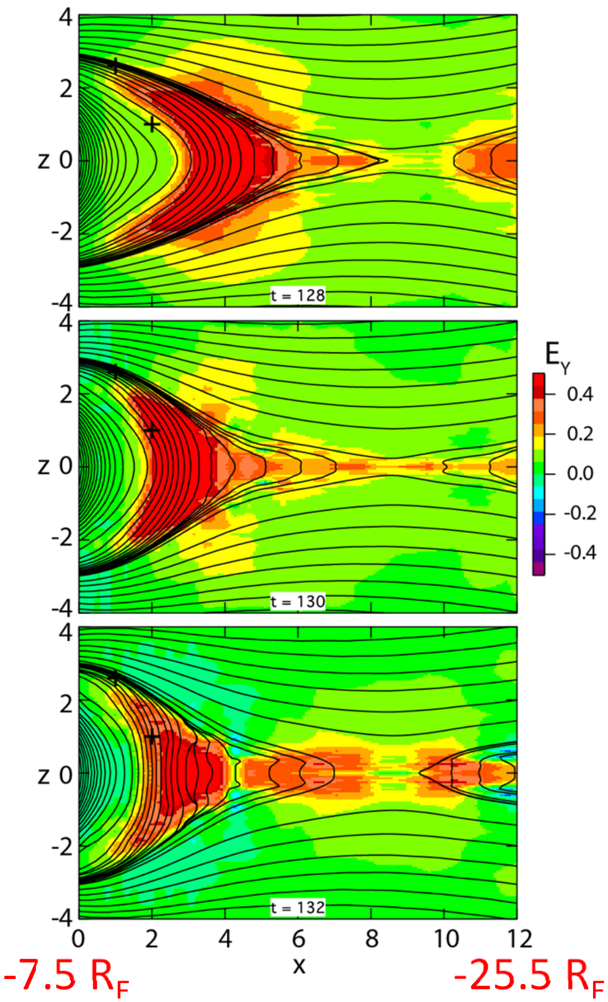

B-field, omni-directional energy fluxes

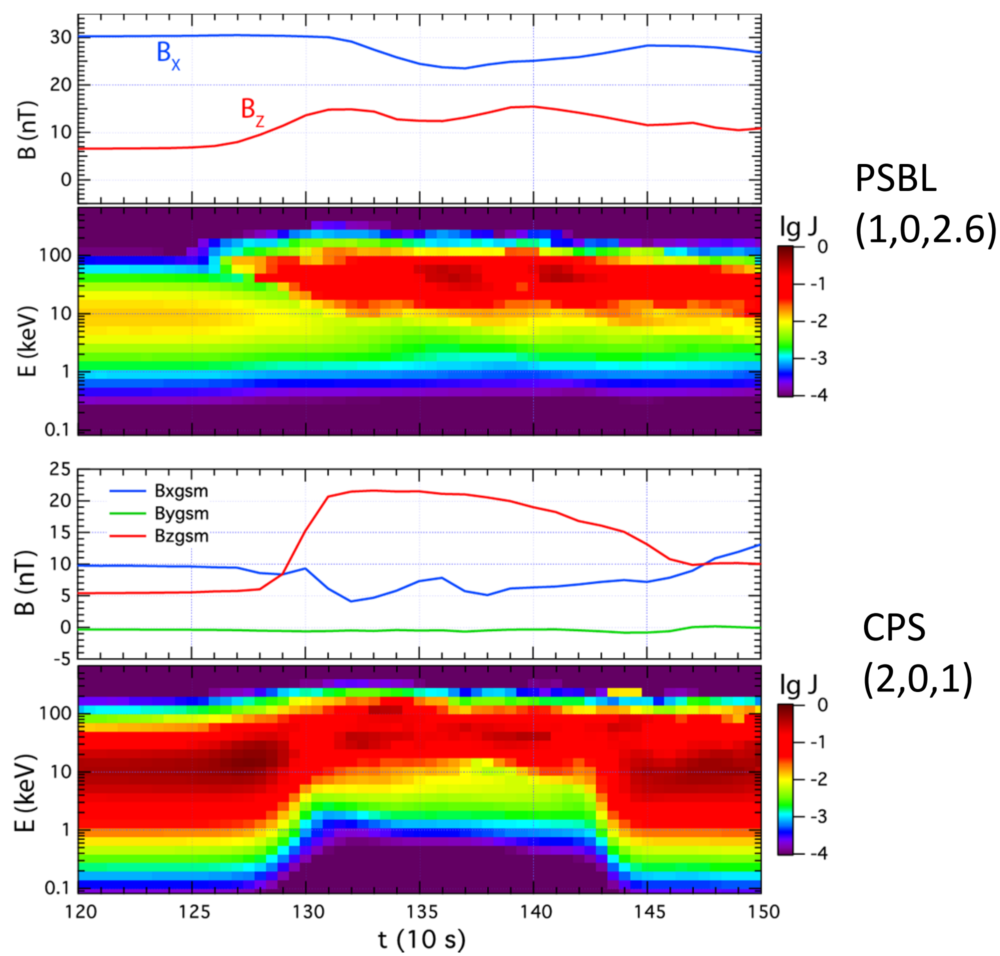

CPS, omnidirectional proton fluxes

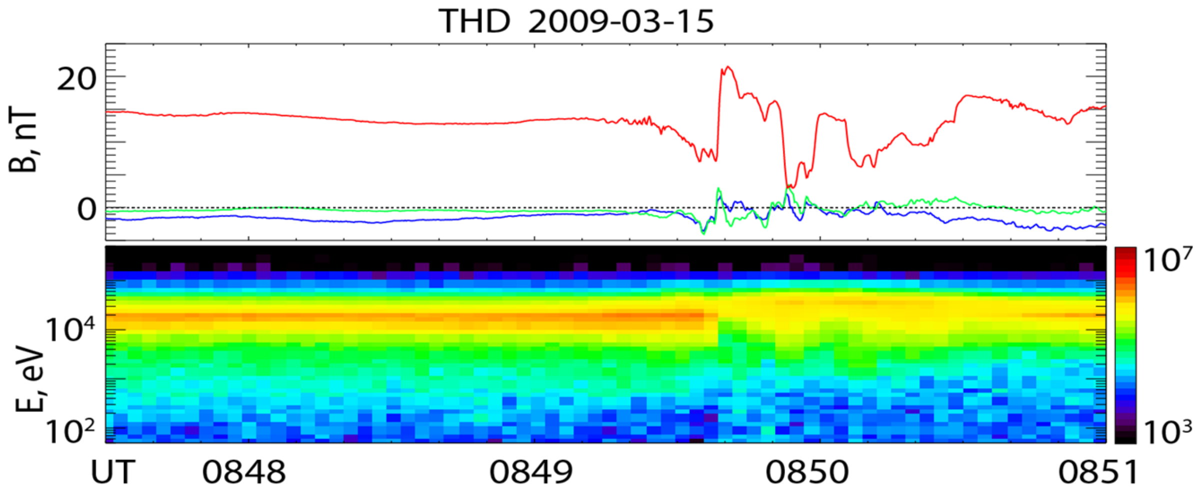

THEMIS observations
(court.: A. Runov)

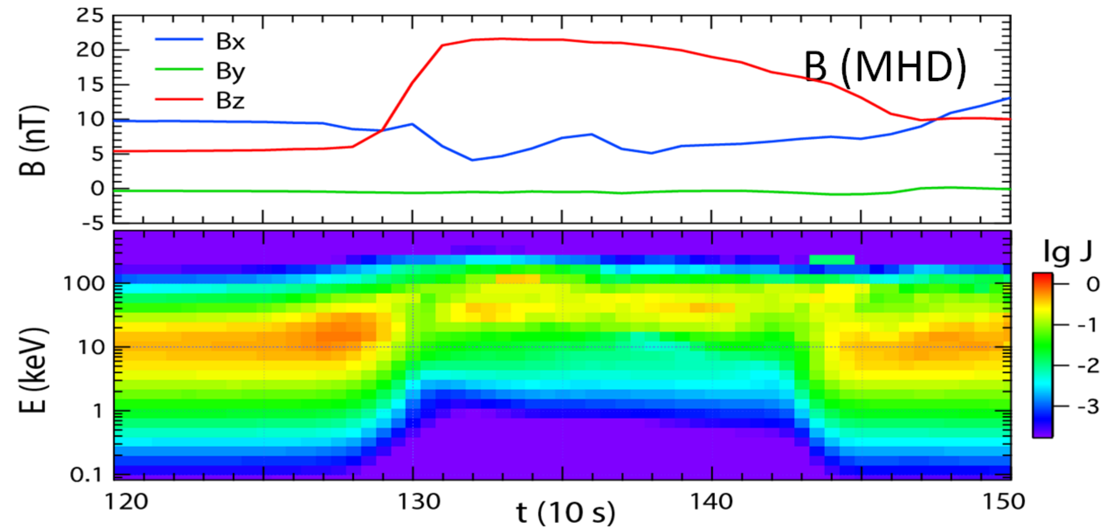

simulations

Ey (MHD)

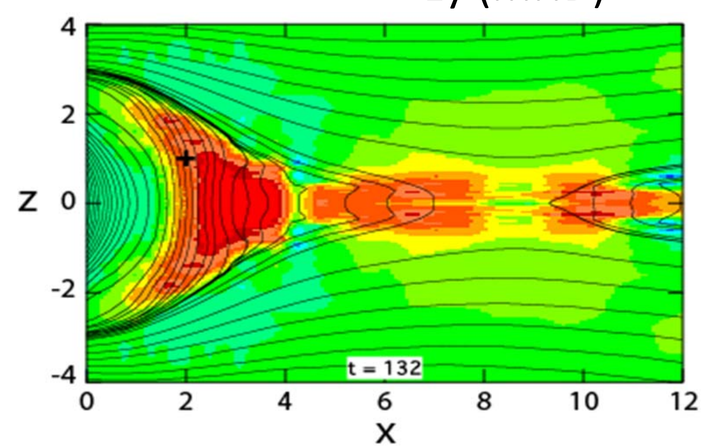

CPS, Proton Velocity Distributions

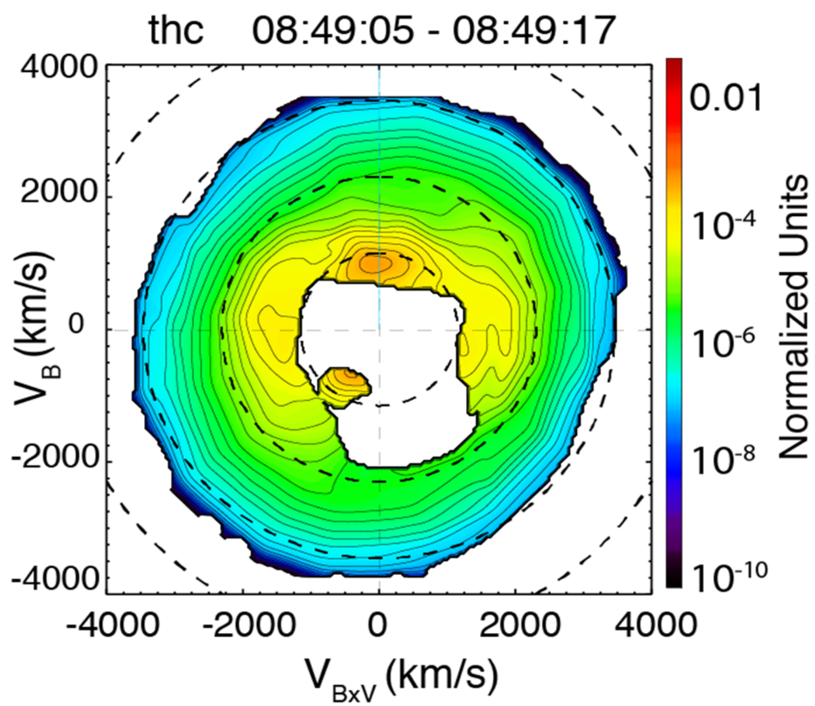

THEMIS observations
(court. A. Runov)

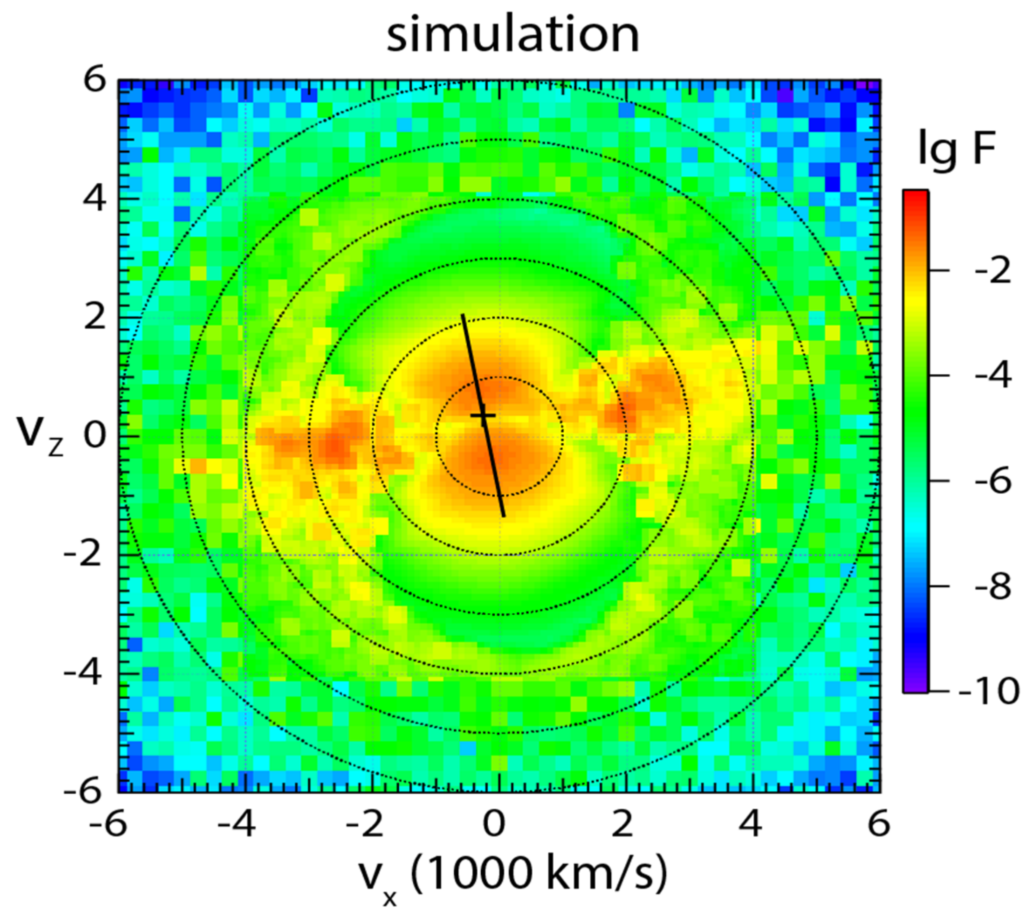

Earthward

CPS Ion Distributions

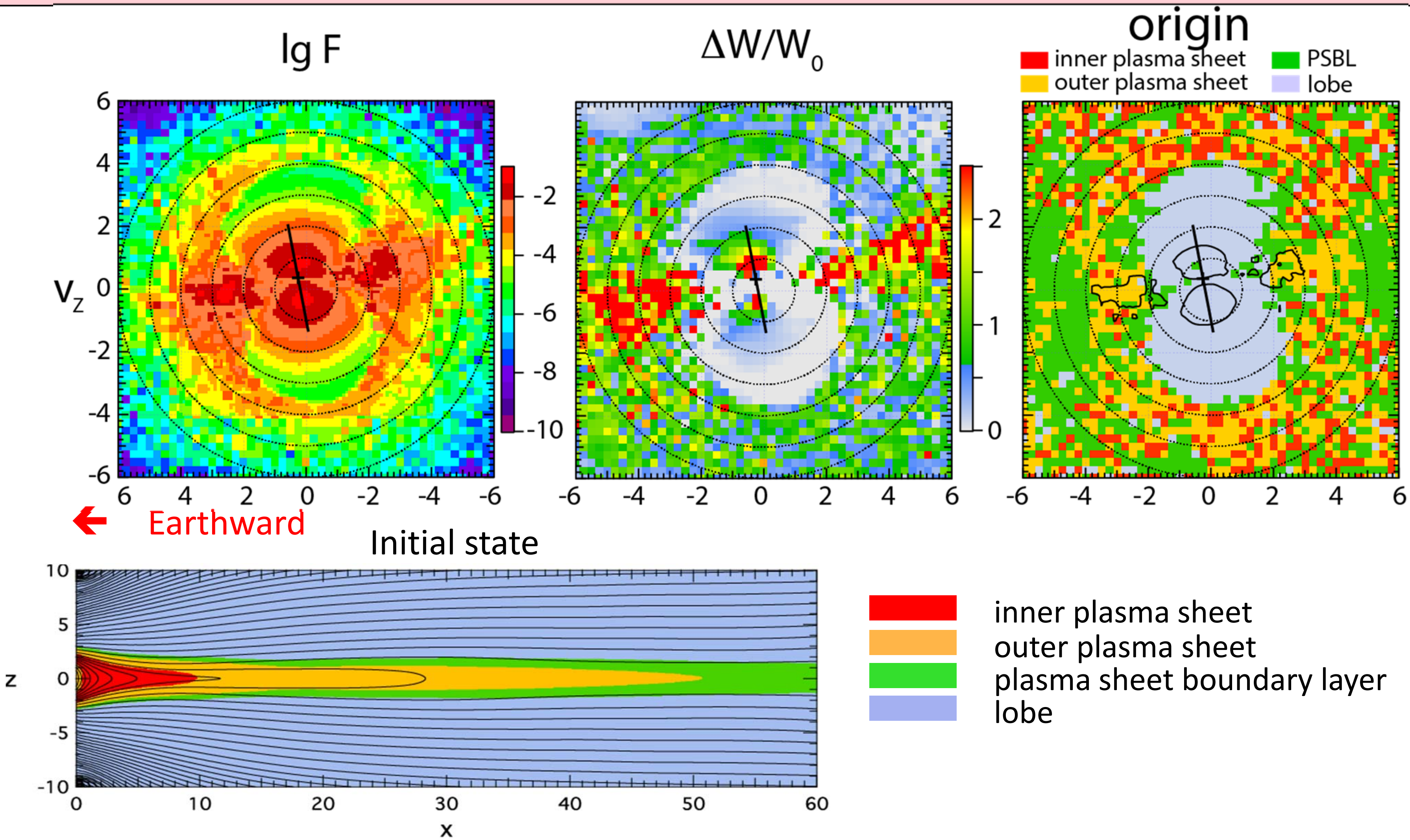

Characteristic CPS Proton Beam Orbit

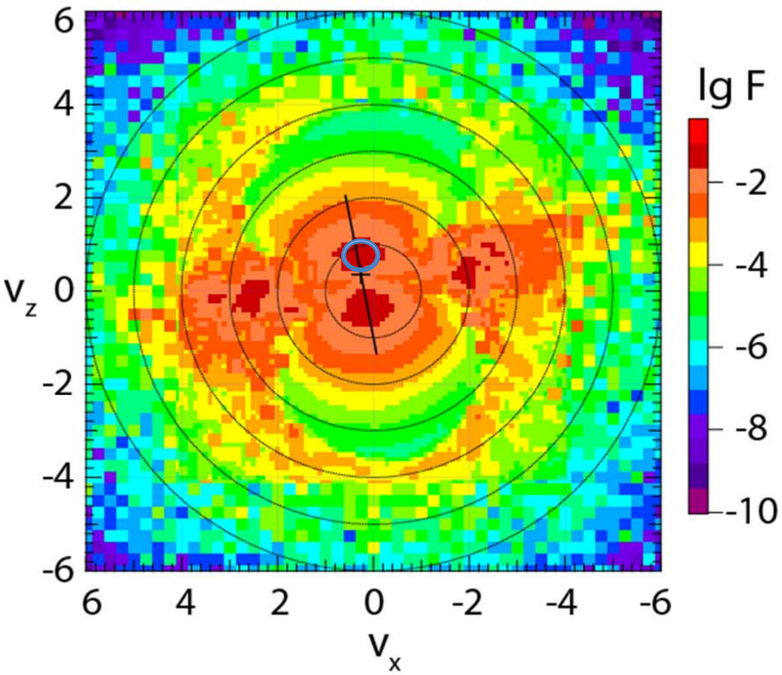

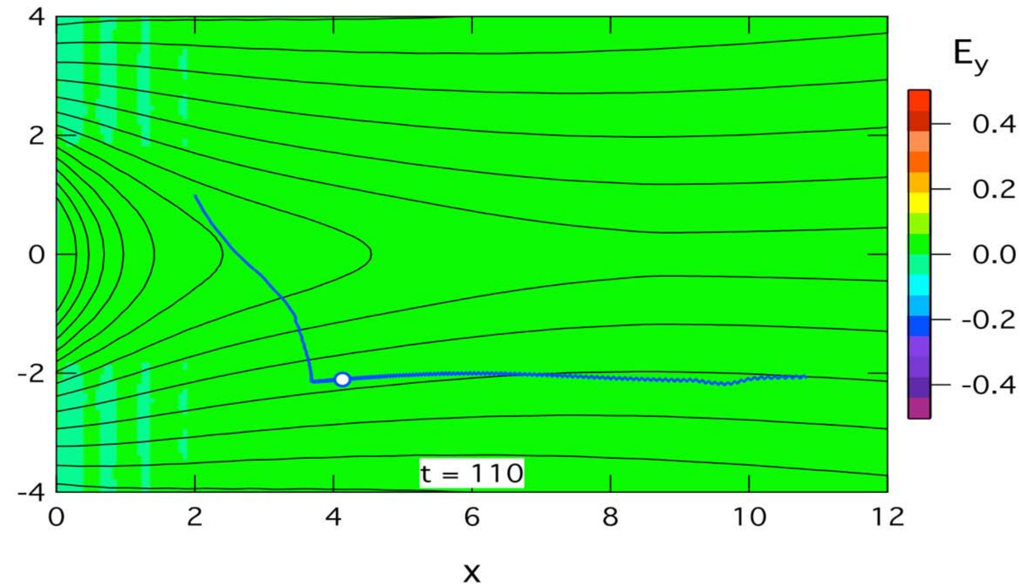

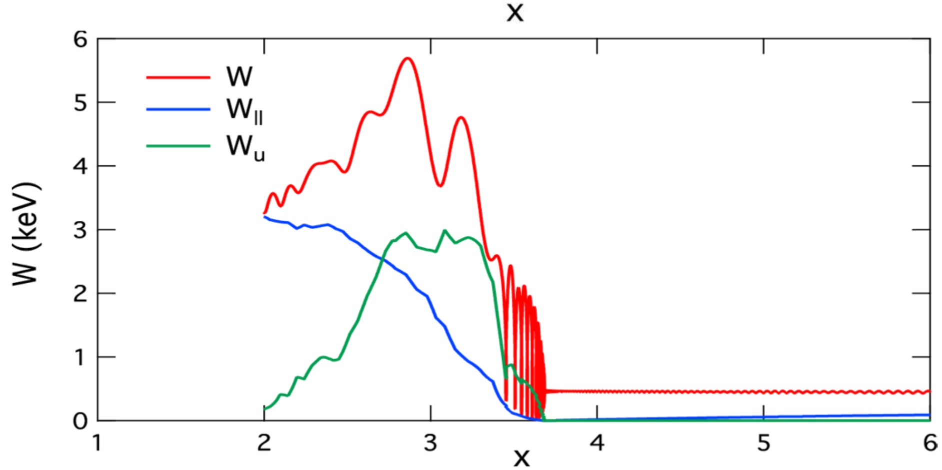

Characteristic Ring Orbit, CPS

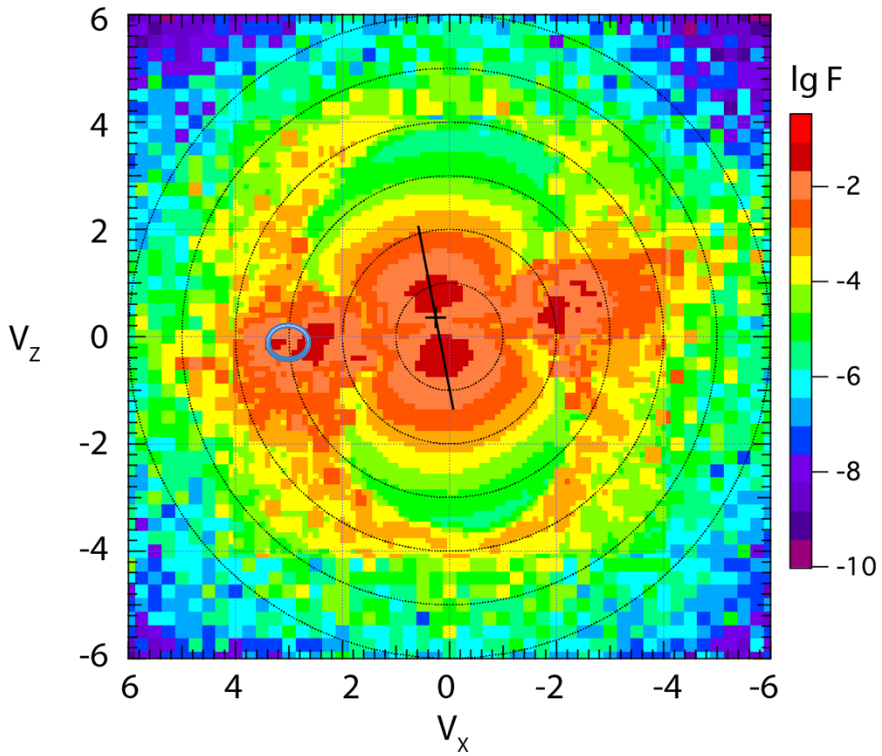

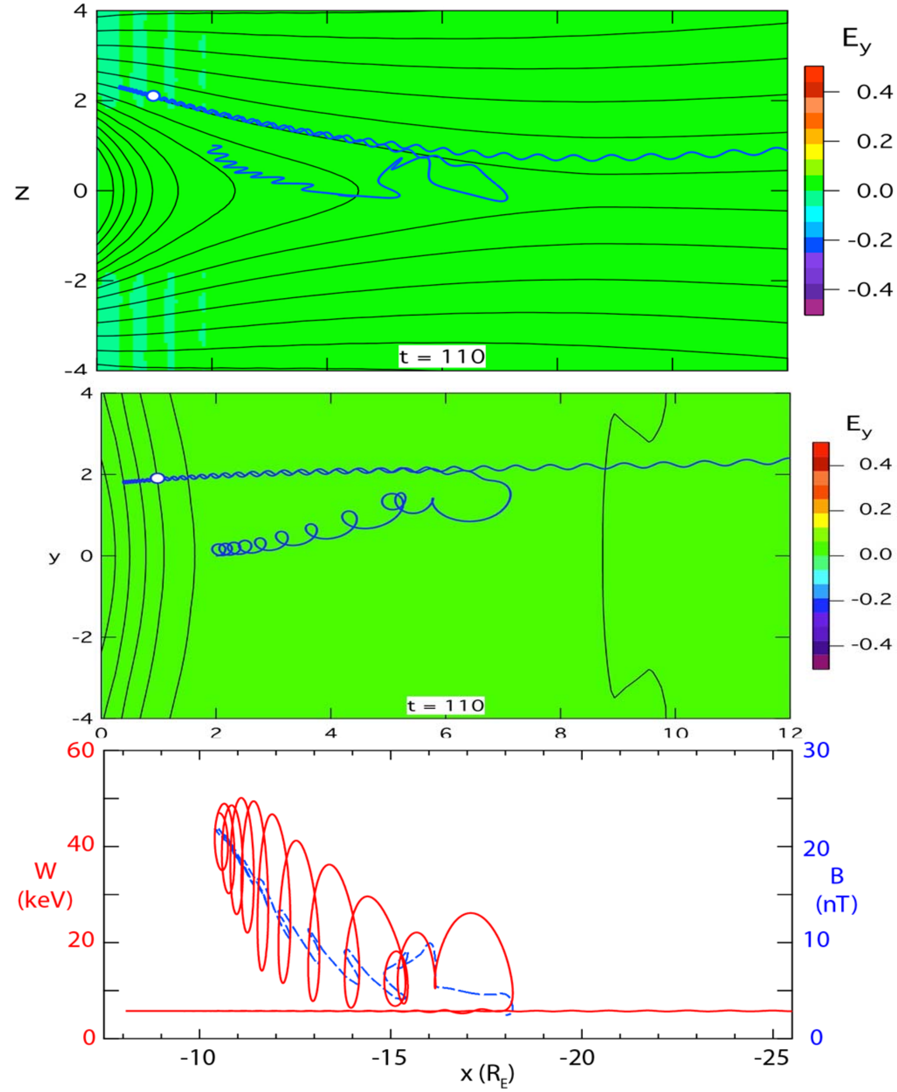

Event 16 July, 2017: Entry From the Lobe

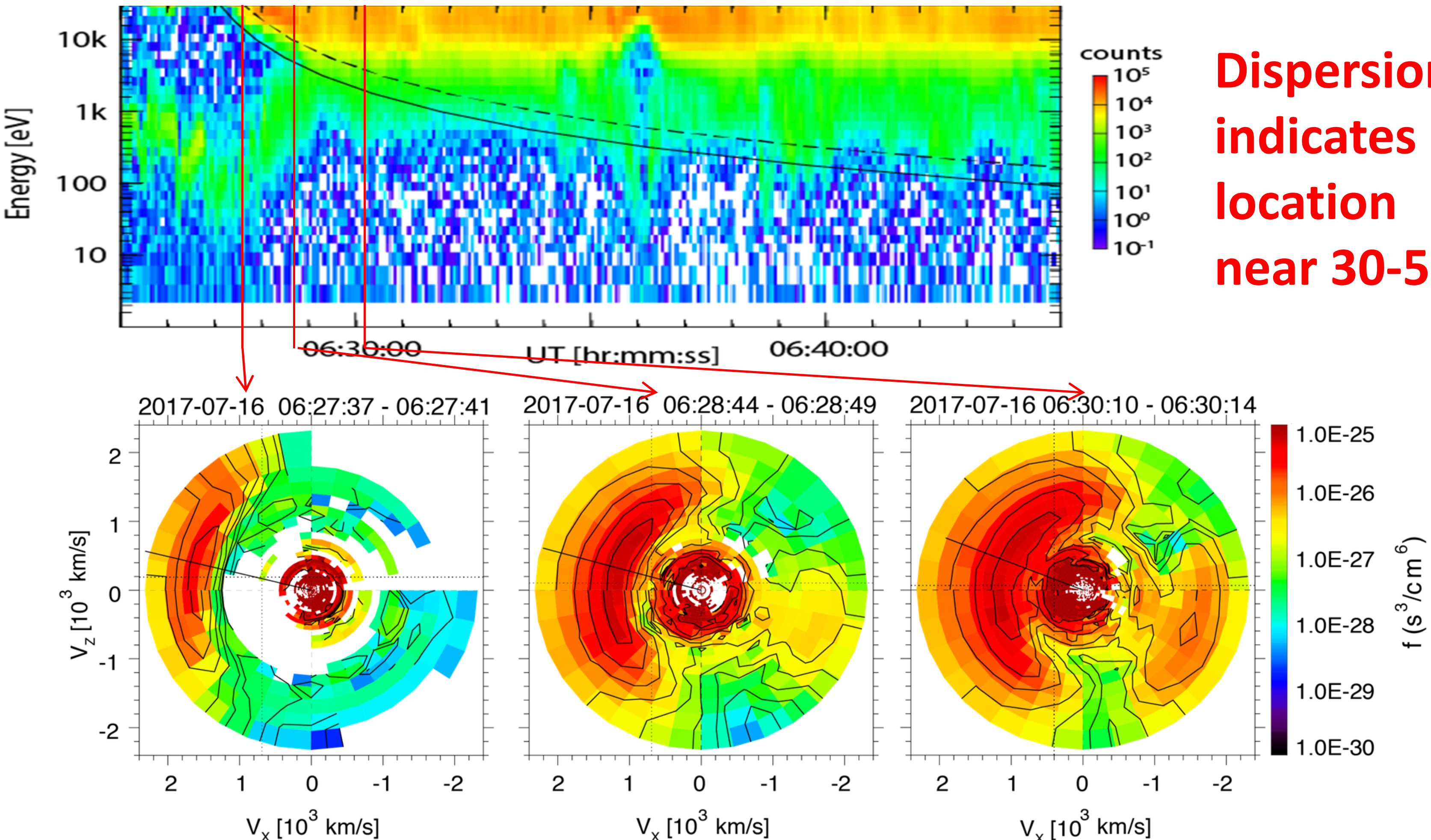

Dispersion indicates source location near 30-50 R_E

(similar to earlier ISEE observations by Forbes et al., 1981)

Observed & Simulated Ion Beam Distributions, PSBL

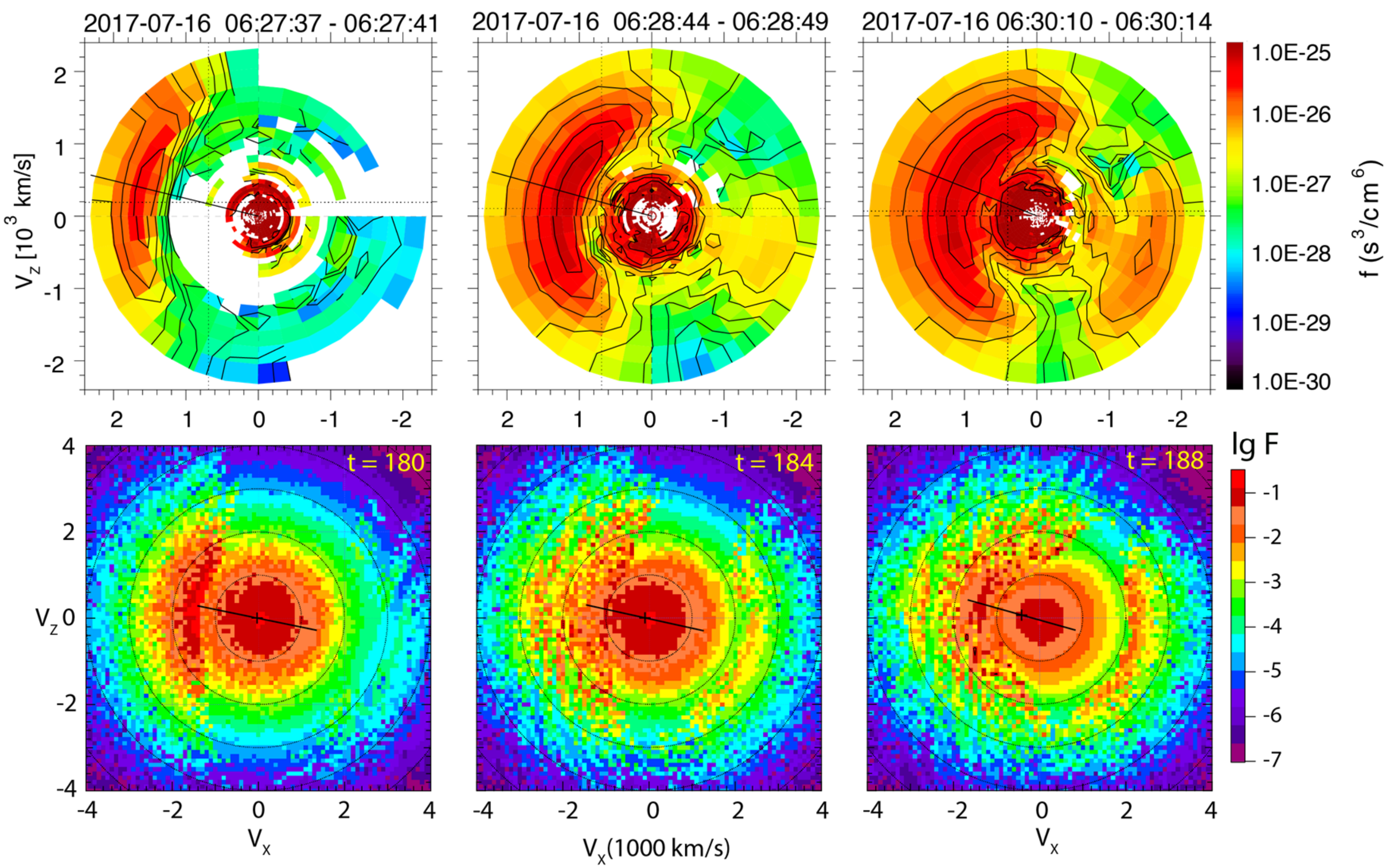

MMS observations (M. Chandler, R. Nakamura)

simulation

← Earthward

Ion PSBL Beam Orbits

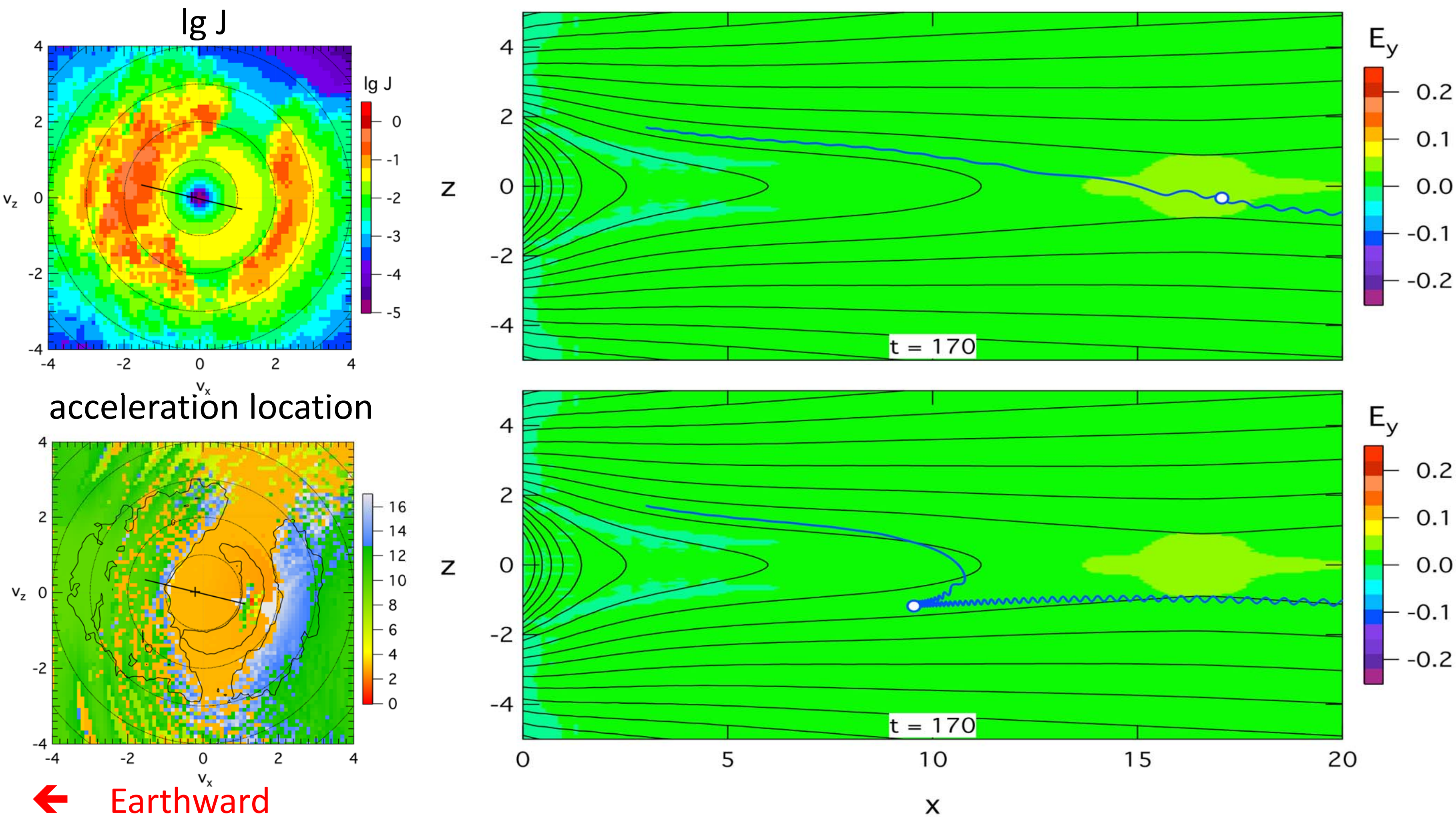

Summary: Ion Distributions in the PSBL and CPS

Good agreement of simulated and observed distributions indicates that cross-tail electric field, modeled by MHD, is the main property accelerating ions and shaping distribution functions

PSBL:

Beams from direct acceleration (x-line, DF) and mirroring near Earth.

Low-energy edge of direct and reflected beams may permit identification of x-line source location (Onsager approach).

(Multiple beams from multiple DF encounters with mirroring)

CPS:

Ring population (perp. anisotropy) from betatron-type acceleration, entry from far plasma sheet via reconnection

Field-aligned beams from current sheet (1st order Fermi) acceleration, entry via ExB drift from near lobe